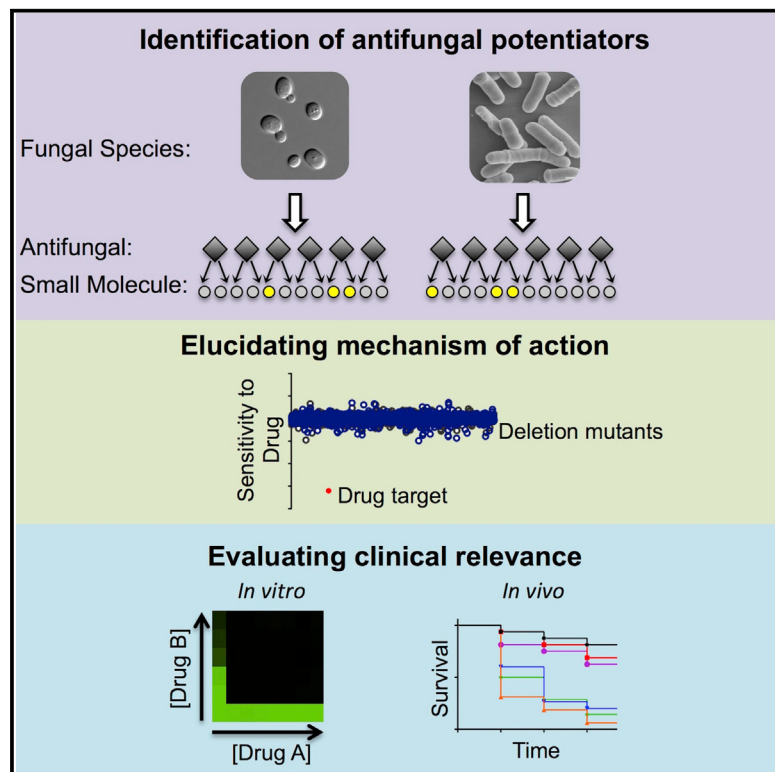


## An Antifungal Combination Matrix Identifies a Rich Pool of Adjuvant Molecules that Enhance Drug Activity against Diverse Fungal Pathogens

### Graphical Abstract



### Authors

Nicole Robbins, Michaela Spitzer,  
Tennison Yu, ..., Donald C. Sheppard,  
Mike Tyers, Gerard D. Wright

### Correspondence

wrightge@mcmaster.ca

### In Brief

There is a dire need for new antifungal therapies. To address this necessity, Robbins et al. screened ~86,000 unique chemical combinations for activity against fungi. The authors find that the antimycobacterial drug clofazimine increases the efficacy of antifungals by disrupting membrane integrity. This study unveils a rich dataset for antifungal development.

### Highlights

- The Antifungal Combination Matrix reports 1,550 antifungal drug combinations
- ACM combinations act against fungal pathogens including azole-resistant *C. albicans*
- Clofazimine potentiates antifungals in diverse fungi by targeting membrane function
- Clofazimine potentiates caspofungin in an invertebrate model of fungal pathogenesis



# An Antifungal Combination Matrix Identifies a Rich Pool of Adjuvant Molecules that Enhance Drug Activity against Diverse Fungal Pathogens

Nicole Robbins,<sup>1</sup> Michaela Spitzer,<sup>1</sup> Tennison Yu,<sup>1</sup> Robert P. Cerone,<sup>2</sup> Anna K. Averette,<sup>5</sup> Yong-Sun Bahn,<sup>6</sup> Joseph Heitman,<sup>5</sup> Donald C. Sheppard,<sup>3</sup> Mike Tyers,<sup>4</sup> and Gerard D. Wright<sup>1,\*</sup>

<sup>1</sup>Michael G. DeGroote Institute for Infectious Disease Research and the Department of Biochemistry and Biomedical Sciences, McMaster University, Hamilton, ON L8N 3Z5, Canada

<sup>2</sup>Department of Microbiology and Immunology, McGill University, Montréal, QC H3G 1A4, Canada

<sup>3</sup>Department of Medicine, McGill University, Montréal, QC H3G 1A4, Canada

<sup>4</sup>Institute for Research in Immunology and Cancer, Université de Montréal, Pavillon Montréal, QC H3C 3J7, Canada

<sup>5</sup>Departments of Molecular Genetics and Microbiology, Medicine, and Pharmacology and Cancer Biology, Duke University Medical Center, Durham, NC 27710, USA

<sup>6</sup>Department of Biotechnology, College of Life Science and Biotechnology, Yonsei University, Seoul 120-749, Republic of Korea

\*Correspondence: [wrightge@mcmaster.ca](mailto:wrightge@mcmaster.ca)

<http://dx.doi.org/10.1016/j.celrep.2015.10.018>

This is an open access article under the CC BY-NC-ND license (<http://creativecommons.org/licenses/by-nc-nd/4.0/>).

## SUMMARY

There is an urgent need to identify new treatments for fungal infections. By combining sub-lethal concentrations of the known antifungals fluconazole, caspofungin, amphotericin B, terbinafine, benomyl, and cyprodinil with ~3,600 compounds in diverse fungal species, we generated a deep reservoir of chemical-chemical interactions termed the Antifungal Combinations Matrix (ACM). Follow-up susceptibility testing against a fluconazole-resistant isolate of *C. albicans* unveiled ACM combinations capable of potentiating fluconazole in this clinical strain. We used chemical genetics to elucidate the mode of action of the antimycobacterial drug clofazimine, a compound with unreported antifungal activity that synergized with several antifungals. Clofazimine induces a cell membrane stress for which the Pkc1 signaling pathway is required for tolerance. Additional tests against additional fungal pathogens, including *Aspergillus fumigatus*, highlighted that clofazimine exhibits efficacy as a combination agent against multiple fungi. Thus, the ACM is a rich reservoir of chemical combinations with therapeutic potential against diverse fungal pathogens.

## INTRODUCTION

Fungal pathogens have emerged as a leading cause of human mortality. Current estimates suggest death due to invasive fungal infections is on par with more well-known infectious diseases such as tuberculosis (Brown et al., 2012; Denning and Bromley, 2015), with costs to the health care system of ~\$2.6 billion annu-

ally in the United States alone (Wilson et al., 2002). These staggering clinical and economic impacts are in large part due to the limited number of validated cellular targets available in fungi to exploit for drug discovery, and the ability of fungal pathogens to thwart therapeutic regimens by evolving resistance to current treatments. *Candida albicans*, *Cryptococcus neoformans*, and *Aspergillus fumigatus* represent the most prevalent fungal pathogens of humans (Brown et al., 2012). Each of these species is responsible for hundreds of thousands of infections annually with unacceptably high mortality rates due to poor diagnostics and limited treatment options (Brown et al., 2012). Furthermore, the rapid emergence of drug resistance in *Candida* species poses a serious threat to human health as identified by the Centers for Disease Control and Prevention (2013). The challenge that remains in the medical mycology community is the identification of therapies with efficacy against fungal pathogens while maintaining minimal human toxicity.

A limited number of antifungal drugs exhibit selective toxicity to fungi because of the evolutionary conservation of eukaryotic gene function from fungi to humans. The polyenes, which cause severe nephrotoxicity, form large extramembranous aggregates that extract the essential membrane-lipid ergosterol from the plasma membrane (Anderson et al., 2014). The azoles inhibit ergosterol biosynthesis and impede cellular growth, but because these compounds are merely fungistatic resistance is readily acquired. The only new class of antifungal to reach the clinic in decades is the echinocandins, which inhibit synthesis of  $\beta$ -(1,3) glucan, a key component of the fungal cell wall (Ostrosky-Zeichner et al., 2010). This paucity of fungal-specific targets is problematic given the prevalence of cross-resistance to all drugs with a common target, and indeed resistance to all widely deployed antifungals has been documented in both the laboratory and the clinic (Shapiro et al., 2011).

Despite efforts over the past several decades to discover novel treatments for fungal infections, there remains a paucity of new drug leads and new drug targets. Recent efforts to understand

the complex networks that underpin the biology of fungi in model species suggest new therapeutic strategies. Large-scale genetic and proteomic studies in the budding yeast *Saccharomyces cerevisiae* have revealed that cellular behavior is controlled by a highly interconnected and functionally redundant network of gene and protein interactions (Costanzo et al., 2010; Sharom et al., 2004). While only ~1,000 of the ~6,000 genes in *S. cerevisiae* are essential for growth, systematic efforts to simultaneously disrupt any two non-essential genes in the same cell has revealed over 170,000 synthetic lethal combinations (Costanzo et al., 2010). This redundancy, referred to as genetic buffering, in part explains the difficulty of identifying single compounds that result in cellular toxicity. The vast network of synthetic lethal genetic interactions represents an untapped target space for drug discovery, as, in principle, combinations of compounds that perturb fungal genetic networks at two or more nodes may result in selective toxicity. Furthermore, combinatorial inhibition can confer enhanced efficacy and specificity compared to individual drug treatments and can slow the evolution of resistance (Zimmermann et al., 2007). Ad hoc drug combinations discovered by trial and error have been widely used against many diseases. For example, the current gold standard antifungal regimen for cryptococcal meningitis is a combination of amphotericin B and 5-flucytosine (Day et al., 2013). The systematic discovery of active drug combinations to treat fungal infections, predicated on the concept of extensive genetic network redundancy, is a potentially rich source of new antifungal agents.

The re-purposing of previously approved drugs for new indications has emerged as one means to expedite drug development because the known toxicology and pharmacology lowers regulatory barriers and cost. The combination of established antifungals with re-purposed drugs from other indications holds considerable promise. In an early example, calcineurin or target of rapamycin (TOR) inhibitors improved the efficacy of fluconazole against a variety of pathogenic fungi (Blankenship et al., 2003). More recently, the Hsp90 inhibitor 17-AAG was found to synergize with fluconazole against *C. albicans* in a *Galleria mellonella* model of systemic candidiasis, and in a rat catheter model of biofilm infection (Cowen et al., 2009; Robbins et al., 2011). A large-scale systematic analysis of chemical-chemical interactions identified 148 bioactive molecules that potentiate the activity of fluconazole toward diverse fungal species, including clinical pathogens (Spitzer et al., 2011). Another screen of off-patent drugs revealed 15 compounds with activity against *C. neoformans* (Butts et al., 2013). High-throughput screens for synergistic enhancers of known antifungal agents thus have the potential to yield effective combination therapeutics against clinically relevant pathogens.

In this study, we screened sub-lethal concentrations of six known antifungals in combination with ~3,600 different bioactive compounds to uncover synergistic drug combinations. Parallel screens were performed in the model yeasts *S. cerevisiae* and *Schizosaccharomyces pombe*, as well as in the fungal pathogens *C. albicans* and *C. neoformans* to generate the most comprehensive analysis of drug combinations in fungi to date. This dataset of drug interactions, which we have termed the Antifungal Combination Matrix (ACM), contains hundreds

of chemical combinations that abrogate fungal growth, often in an antifungal- and species-specific manner. We show that a number of antifungal combinations are active toward an isolate of *C. albicans* that had acquired fluconazole resistance in the clinic. Chemical-genetic profiling of clofazimine, an antimycobacterial agent for which antifungal activity has not been described, suggested that it induces a Pkc1-dependent cell membrane stress response. We further show that clofazimine is a general potentiator of antifungal activity in fungal species separated by ~1 billion years of evolution. Thus, the ACM represents a unique resource of chemical probes for the study of fungal biology, and an entry point for discovery of combination therapeutics against diverse fungal pathogens.

## RESULTS

### The Antifungal Combination Matrix

To identify molecules that potentiate known antifungal agents, we selected six entry-point drugs. We chose four clinically relevant drugs with well-characterized targets: amphotericin B (ergosterol, cell membrane), fluconazole (Erg11; ergosterol biosynthesis), terbinafine (Erg1; ergosterol biosynthesis), and caspofungin ( $\beta$ -glucan synthase, cell wall synthesis). We also selected two agricultural fungicides: benomyl, a microtubule inhibitor, and cyprodinil, a compound whose mode of action remains enigmatic. High-throughput combination screens were performed against four different fungal species: *S. cerevisiae*, *S. pombe*, *C. albicans*, and *C. neoformans*. These evolutionarily divergent genera were chosen in order to identify combination agents in model yeast species where mode of action can be readily probed using advanced functional genomic reagents, and in clinically relevant fungal pathogens. Each species was screened using compounds from the McMaster Bioactives collection, a library of ~3,600 unique small molecules derived from commercial sources. All of the screens were performed with 12.5  $\mu$ M of compound in the absence and presence of 1/4 minimum inhibitory concentration (MIC) of the antifungal drug (Table S1). This concentration regimen enabled identification of antifungal potentiators that had minimal growth effects on their own. Residual activity was calculated for each compound, and data were normalized for plate- and row/column-specific effects as described previously (Table S2) (Spitzer et al., 2011). Compounds that were greater than three median absolute deviations (MADs) below the diagonal had less than 50% reduction of growth on their own and resulted in greater than 80% growth inhibition in the presence of antifungal were chosen for further analysis (Figure S1). This dataset called the antifungal combination matrix (ACM) contained over 228,000 data points for ~86,000 unique pairwise chemical-chemical interactions and identified 1,550 drug combinations that showed efficacy against at least one fungal species (Figure 1; Table S3). The ACM represents the largest high-throughput screening effort for combination agents against model yeasts and pathogenic fungi.

To evaluate how the 1,550 active compounds identified in the ACM are related to one another, we displayed the hits as a comprehensive network of chemical-chemical interactions that connect each antifungal entry-point drug to the chemicals

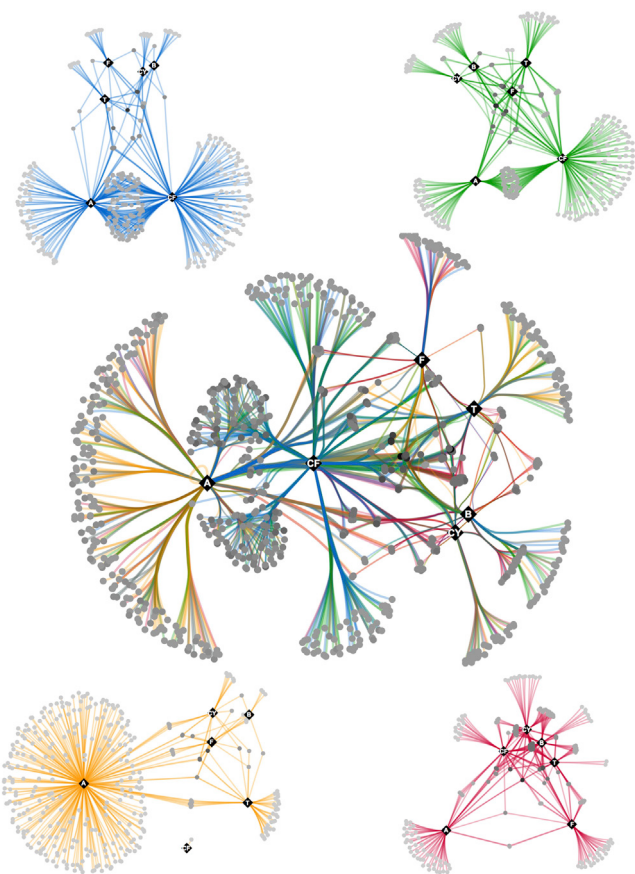


**Figure 1. The ACM Chemical-Chemical Interaction Network**

The central chemical-chemical interaction network comprises a total of 1,550 chemical interactions. Compounds that potentiated an antifungal are depicted as circles and are connected by edges to the antifungal in which synergy is observed. Edges are colored to represent interactions identified against different fungal species with blue representing *C. albicans*, green representing *S. cerevisiae*, orange representing *C. neoformans*, and red representing *S. pombe*. Antifungals are shown as black diamonds. (Amphotericin B [A], benomyl [B], caspofungin [CF], cyprodinil [CY], fluconazole [F], or terbinafine [T]). Chemical-chemical networks for each individual species are plotted in corners and are colored as described above. See also Figures S1 and S2 and Tables S1, S2, and S3.

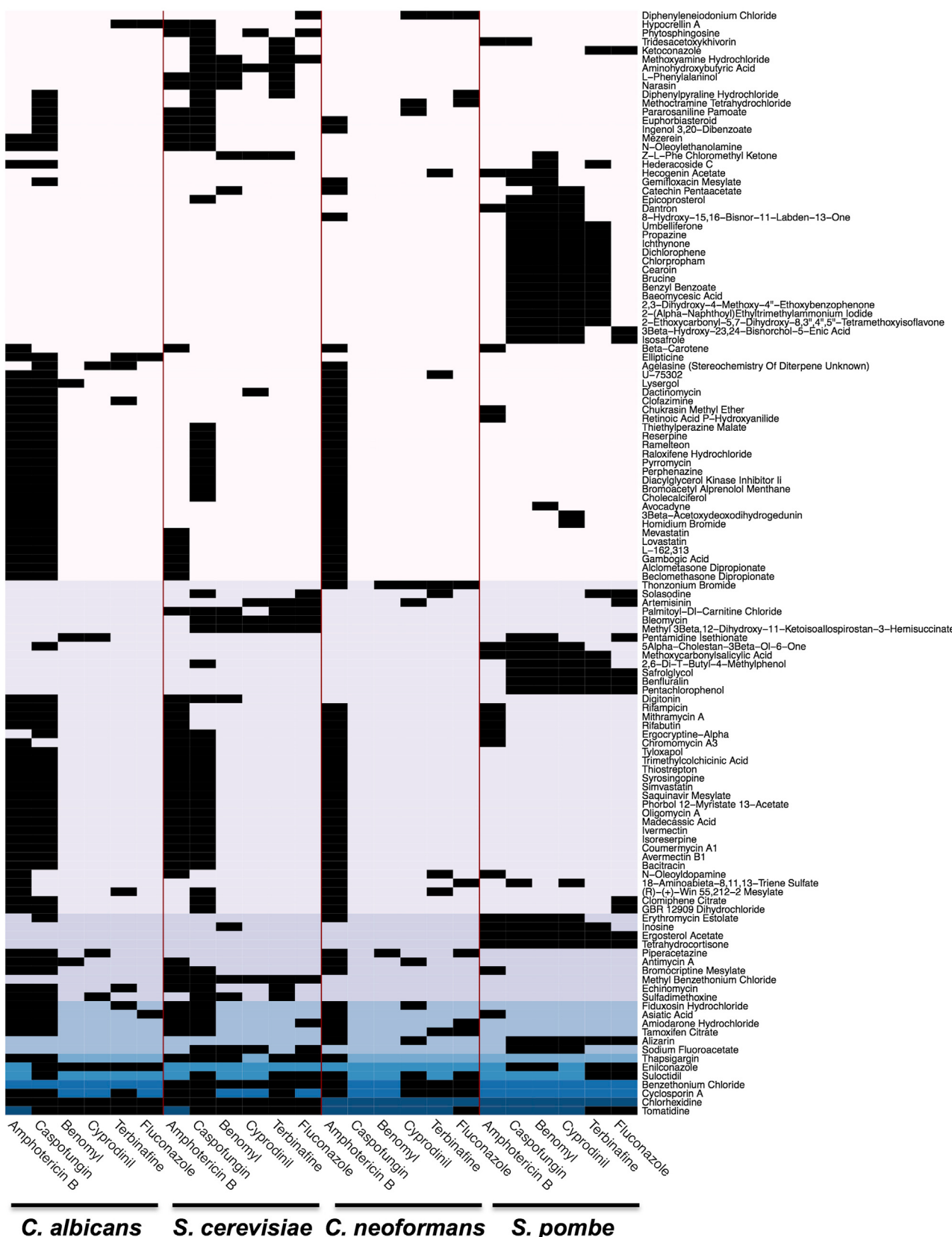
that were screened as a function of the species in which the interaction was identified (Figure 1). This unveiled an intricate pattern of chemical-chemical combinations capable of abrogating fungal growth. Different screens had dramatically different numbers of compounds that increased the efficacy of each antifungal agent, with hit rates as high as 7.4% for the amphotericin B screen performed in *C. neoformans* and as low as 0.18% for the benomyl screen performed in *C. neoformans* (Figure 1). These hit rates were within the range reported from other drug combination screens (Boris et al., 2003; Spitzer et al., 2011). More potentiators were identified with the antifungals caspofungin and amphotericin B, which disrupt cell wall or membrane (Figure 1). Benomyl, cyprodinil, fluconazole, and terbinafine had markedly fewer hits that were more drug specific (Figures 1 and S2), demonstrating different antifungal classes elicit

dramatically different rates of potentiation with other small molecules.

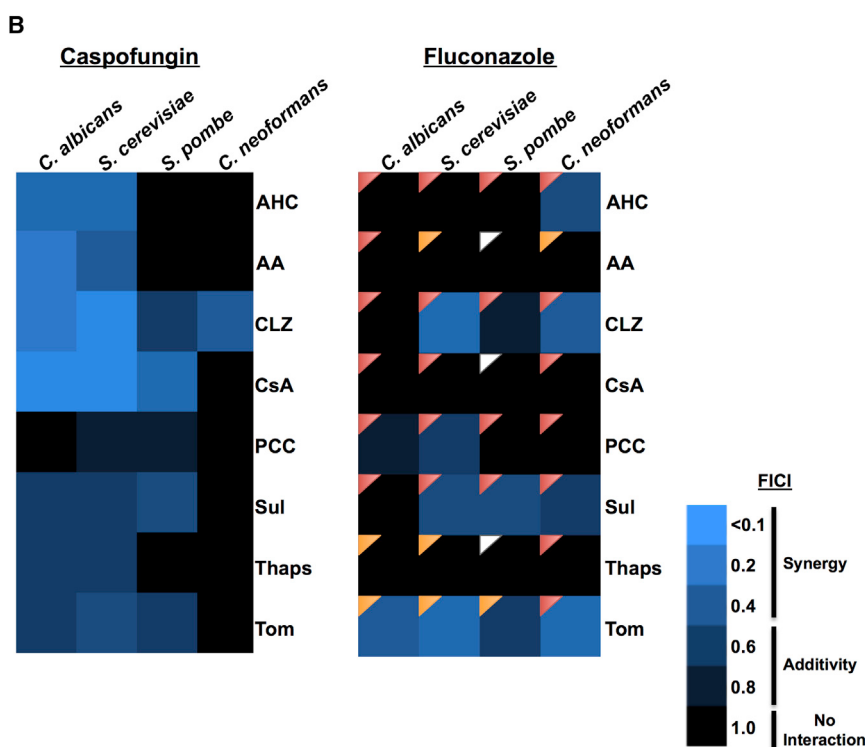
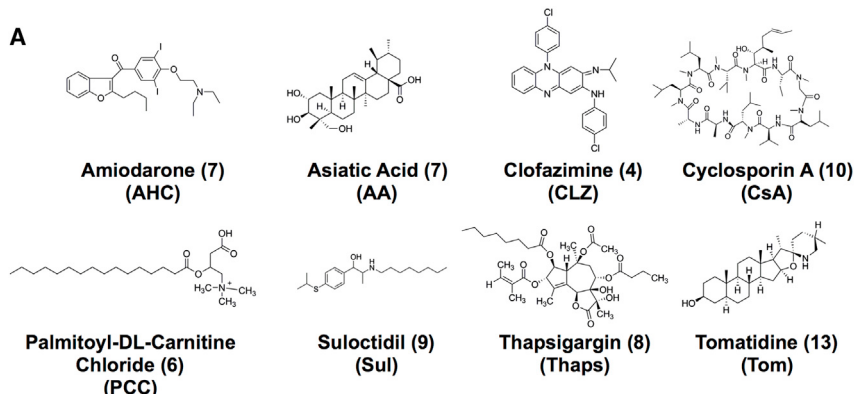
The vast majority of the hits in the ACM were species and/or antifungal specific, with only 22 compounds identified in more than five screens. We visualized all compounds in a heatmap to reveal the specific conditions linked by these “high-connectivity” compounds (Figure 2). Small molecules that were identified most frequently as potentiators included tomatidine and chlorhexidine, identified in 13 and 12 screens, respectively. Notably, both of these molecules are reported membrane perturbing agents (Gilbert and Moore, 2005; Simons et al., 2006). Separate chemical-species interaction networks for each antifungal drug revealed species-specific effects elicited by a majority of the combination treatments explored (Figure S2). For example, molecules that increased the efficacy of fluconazole, terbinafine, benomyl, and cyprodinil were largely antifungal specific with little overlap across the different fungal species (Figure S2). In contrast, when examining potentiators of amphotericin B, *C. neoformans* and *C. albicans* shared the largest number of hits, whereas *C. albicans* and *S. cerevisiae* shared a high number of caspofungin potentiators (Figure S2). In addition, *C. albicans* and *S. cerevisiae* both had a high number of compounds that increased the efficacy of both amphotericin B and caspofungin (Figure 1). Overall, the ACM represents an extensive resource of bioactive chemical space for antifungal drug discovery.

#### Hit Validation and Characterization

To explore a subset of the 1,550 hits from the ACM, we chose eight compounds for additional drug susceptibility analysis. These eight compounds were chosen based on diversity of chemical class (Figure 3A), therapeutic use when known, and the screens in which they were identified (Table S4). We tested these eight compounds using standard concentration matrix (checkerboard) assays in combination with the clinically relevant antifungals caspofungin or fluconazole (Figure S3). Data were quantified by calculation of the fractional inhibitory concentration index (FICI), an accepted method for evaluating chemical interactions in infectious disease (Figure 3B) (Odds, 2003). Drug interactions are synergistic if the calculated FICI is below of 0.5, additive if the FICI is 0.5–0.99 and an FICI between 1.0 and 4.0 indicates no chemical-chemical interaction (Odds, 2003). Amiodarone hydrochloride, asiatic acid, clofazimine, and cyclosporin A were synergistic with caspofungin against *C. albicans* and *S. cerevisiae* (Figure 3B; Table S5). Cyclosporin A was also synergistic with caspofungin against *S. pombe*, and clofazimine was synergistic with caspofungin against *C. neoformans* (Figure 3B; Table S5). Checkerboard assays performed with fluconazole revealed tomatidine as a potent synergizer of fluconazole against *C. albicans*, *S. cerevisiae*, and *C. neoformans* (Figure 3B; Table S5). Similarly, clofazimine was synergistic with fluconazole against *S. cerevisiae* and *C. neoformans*. All remaining drug interactions were either additive or showed no interaction (Table S5). In total, 72 checkerboard assays were conducted with drug combinations from the primary screen. All hits from the screens were confirmed except for thapsigargin with fluconazole against *S. cerevisiae* (Figures S3 and S5; Table S4). Overall, these detailed analyses verified interactions identified in the ACM.



(legend on next page)



A limitation of the azoles is that resistance readily evolves due to the fungistatic nature of the drug (Shapiro et al., 2011). To determine whether any compounds rendered fluconazole fungicidal, we used tandem assays with an antifungal susceptibility test followed by spotting onto rich medium without inhibitors. We tested cidal activity for compounds that reduced growth in the presence of fluconazole more so than growth in either drug individually (Figure S3). An overwhelming majority of the chemical-chemical interactions evaluated transformed fluconazole to a fungicidal drug (Figure 3B). These results suggest that the flu-

### Figure 3. ACM Hit Validation and Characterization

(A) Structures of compounds identified as potentiators in the ACM. The numbers shown in brackets indicate the number of screens in which they were identified. See also Table S4.

(B) Heatmap of drug interactions with caspofungin or fluconazole in each species as measured by fractional inhibition concentration index (FICI). Light blue indicates synergistic drug interactions ( $FICI < 0.5$ ); darker shades of blue represent additivity ( $FICI 0.5-0.99$ ); black represents no interaction ( $FICI 1.0-4.0$ ). Compounds tested in combination with fluconazole were examined for cidal activity. Red triangles indicate a fungicidal drug combination, orange triangles indicate fungistatic drug combinations, and white triangles indicate conditions where no inhibition of growth was observed (mitigation testing).

See also Figure S3 and Tables S4 and S5.

conazole enhancers may help suppress the emergence of antifungal resistance.

### Drug Combinations with Efficacy against a *C. albicans* Clinical Isolate

In clinical settings, many thousands of antifungal-resistant infections are diagnosed every year, particularly fluconazole-resistant *C. albicans* (Centers for Disease Control and Prevention, 2013).

Therefore, we evaluated the activity of fluconazole enhancers originally identified in the ACM against a bona fide fluconazole-resistant clinical isolate of *C. albicans*. This strain had a fluconazole MIC of 128 µg/ml, ~250-fold higher than the laboratory strain likely due to mutations identified in the azole target *ERG11* (*Erg11*<sup>R264K</sup>), as well as in *TAC1* (*Tac1*<sup>T225A</sup>), a transcriptional activator of ABC transporters. Of the 18 molecules tested, three increased the susceptibility of the resistant clinical

isolate to fluconazole: chlorhexidine, tomatidine, and hypocrellin A (Figure 4A). In order to assess the robustness of these drug interactions, checkerboard assays were conducted, and the FICI was used to evaluate synergy. All three molecules were highly synergistic with fluconazole with FICI values below 0.5 (Figure 4B), unveiling drug combinations with potent activity against a clinically relevant strain of *C. albicans*. Thus, a fraction of antifungal combinations with activity against a wild-type strain of *C. albicans* are able to inhibit the growth of a fluconazole-resistant clinical isolate.

**Figure 2. High-Connectivity Compounds from the ACM**

Those compounds that were identified in four or more screens were visualized on a heatmap. Black rectangles represent conditions where molecules potentiated the antifungal. Background color represents the number of screens in which a molecule was identified with dark blue representing 12 or more screens and light pink representing four screens. The names of compounds that potentiated antifungals are listed on the right and screening conditions are highlighted at the bottom. The heatmap is organized by species and similarity of screening hits. See also Figures S1 and S2 and Tables S2 and S3.

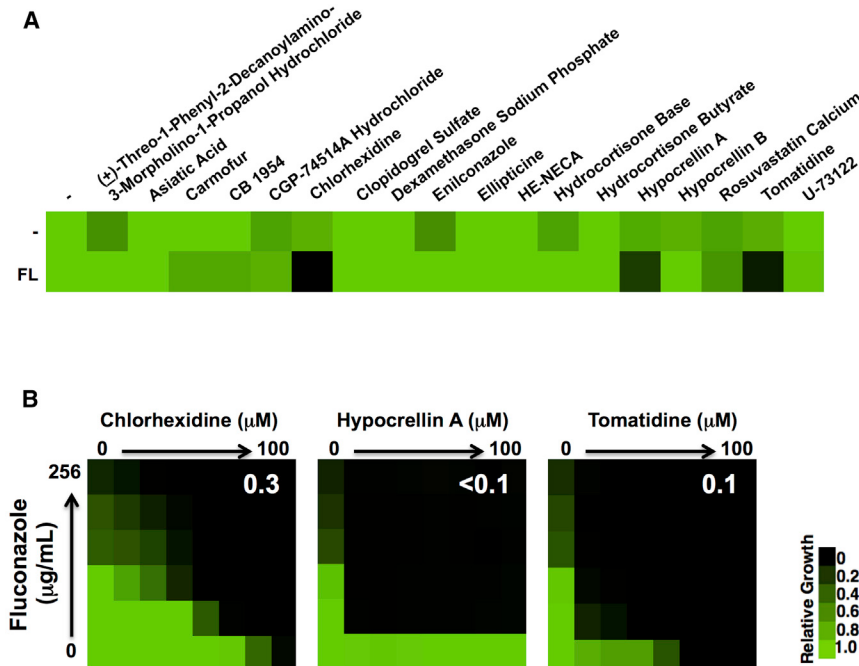


**Figure 4. Drug Combinations with Efficacy against a Clinically Resistant Isolate of *C. albicans***

(A) The 18 compounds identified as potentiators of fluconazole (FL) against *C. albicans* in the ACM were tested against a fluconazole-resistant clinical isolate. *C. albicans* was grown in the absence (–) or presence of 1/4 MIC (32  $\mu\text{g}/\text{ml}$ ) of FL in combination with the ACM hits (12.5  $\mu\text{M}$ ). Growth was measured by OD<sub>600</sub>, and data were quantitatively displayed with color using Treeview (see color bar). (B) Checkerboard assays highlight drug interactions between fluconazole with chlorhexidine, hypocrellin A, or tomatidine. Growth was monitored and analyzed as described in (A). White numbers indicate calculated FICI values.

### Mechanism of Action of Clofazimine

Clofazimine is currently used as an antimycobacterial agent but in our study showed broad-spectrum activity in combination with fluconazole and caspofungin. As clofazimine has not been described as an antifungal, we interrogated the mechanism of action using established genomic profiling methods (Giaever et al., 2004; Pierce et al., 2006). We profiled compound action in haploinsufficiency profiling (HIP) screens, in which the ~1,000 diploid deletion strains heterozygous for essential genes were tested for drug sensitivity to identify candidate compound targets. Genes that encode the target of a compound are expected to be hypersensitive to that compound, as indicated by decreased fitness as measured by competitive growth (Giaever et al., 2004; Pierce et al., 2006). We validated our implementation of this methodology by re-identifying *ERG11* as the established target for fluconazole (Figure S4). The HIP profile generated for clofazimine was distinct from that observed with fluconazole in that a single gene was not markedly more sensitive to clofazimine relative to other genes in the pool. Among the heterozygous mutants most sensitive to clofazimine was *NEO1*, which encodes an essential aminophospholipid translocase required for membrane trafficking and vacuolar biogenesis (Table S6). *NEO1* haploinsufficiency is induced by cationic amphiphilic drugs (CADs) (Lee et al., 2014), a structural feature shared by clofazimine.

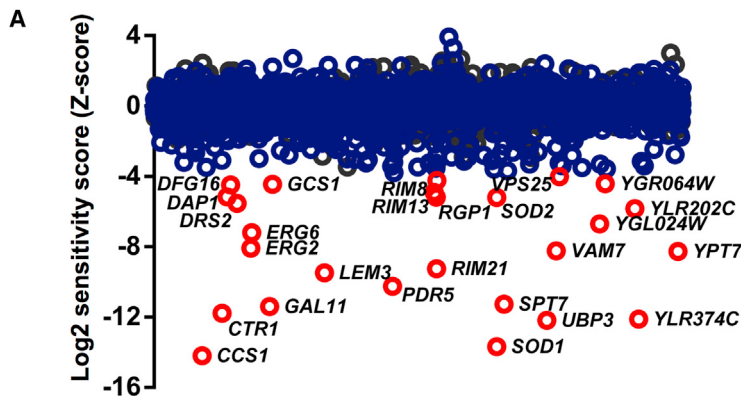
We profiled clofazimine action in homozygous deletion profiling (HOP) screens, in which the ~5,000 deletion strains for non-essential genes were tested for drug sensitivity to identify chemical-genetic interactions indirectly associated with the compound target (Giaever et al., 2004; Pierce et al., 2006). Several gene deletion strains were sensitive to clofazimine including genes important for phospholipid transport, membrane organization, vesicle-mediated transport, and localization (Fig-

ure 5), processes associated with membrane integrity and function (Lee et al., 2014). Moreover, the chemical-genetic profile observed with clofazimine is markedly similar to the structurally related membrane perturbing agent chlorpromazine (De Filippi et al., 2007). In addition, deletion of the copper-related genes

*SOD1*, *CCS1*, and *CTR1* rendered cells sensitive to clofazimine (Figure 5), a feature shared by compounds that elicit high degrees of oxidative stress such as menadione (Lee et al., 2014). Clofazimine sensitivity of the top haploid deletion strains identified in our HOP analysis was confirmed using growth curve analysis (Figure S4). Based on our chemogenomic profile, we postulate that clofazimine may be exerting its effects by disrupting cellular membranes and/or through the generation of reactive oxygen species.

### Clofazimine Induces a Cell Membrane Stress Response and Activates Pkc1

Our chemical-genetic profile implicated a dual mechanism of action for clofazimine. First, we tested our hypothesis that clofazimine elicits a cell membrane stress response. Chlorpromazine and clofazimine are both CADs consisting of a hydrophobic tricyclic ring and a hydrophilic side chain (Figure 6A). The hydrophobic moiety of chlorpromazine allows it to intercalate into the hydrocarbon phase of the membrane bilayer (De Filippi et al., 2007). At physiological pH, the tertiary dimethylpropylamine is protonated and engages in electrostatic interactions with cytosolic anionic lipids (Levin, 2005). Altering in vitro conditions by decreasing the pH of culture medium renders chlorpromazine in its protonated state prior to diffusion across the *S. cerevisiae* membrane, blocking cellular entry and impeding its toxic effects (De Filippi et al., 2007). We tested whether similar effects were observed with clofazimine by spotting wild-type *S. cerevisiae* and a *rim101* mutant, which is hypersensitive to clofazimine, onto agar buffered at pH 5.5 or pH 8. At pH 5.5, cells were resistant to the effects of clofazimine (Figure 6B), presumably due to electrostatic interactions with the cellular membrane that blocked compound entry. At a more basic pH, clofazimine entered the cell and inhibited growth, particularly in the *rim101*



**B**

GO Biological Process Complete	No. Genes Identified in Each Category	No. Genes Expected in Each Category	Fold Enrichment	P-value
phospholipid transport	5	0.3	> 5	2.54E-02
ubiquitin-dependent protein catabolic process via the MVB sorting pathway	5	0.31	> 5	3.17E-02
single-organism membrane organization	15	3.89	3.86	1.34E-02
membrane organization	15	3.95	3.8	1.59E-02
vesicle-mediated transport	18	5.12	3.52	5.20E-03
negative regulation of cellular metabolic process	18	5.94	3.03	3.99E-02
cellular localization	29	12.62	2.3	1.75E-02
single-organism transport	32	15.08	2.12	2.61E-02
transport	37	17.65	2.1	5.04E-03
single-organism localization	34	16.39	2.07	2.01E-02
localization	41	20.05	2.05	1.89E-03
establishment of localization	37	18.22	2.03	1.09E-02
regulation of biological process	42	22.27	1.89	1.15E-02
regulation of cellular process	40	21.4	1.87	2.86E-02
biological regulation	47	25.35	1.85	3.08E-03
single-organism cellular process	67	46.49	1.44	2.58E-02
unclassified	8	10	0.8	0.00E+00

mutant (Figure 6B). This suggests clofazimine interacts with the cellular membrane in a similar manner to chlorpromazine.

Drug-induced phospholipidosis (DIPL) is a phospholipid storage disorder associated with CADs. In yeast, DIPL arises from the selective buildup of CADs in the acidic vacuole; however, loss of acidification reduces intracellular drug accumulation and mitigates toxicity (Anderson and Borlak, 2006). Inhibition of yeast vacuolar adenosine triphosphatase by baflomycin A alleviated the fitness defect induced by clofazimine ( $p < 0.01$ , ANOVA, Bonferroni's multiple comparison test, Figure 6C), in a similar manner to other CADs (Lee et al., 2014), supporting our hypothesis that clofazimine exerts its toxic effects through non-specific membrane perturbations. As high temperature increases turgor pressure and membrane stress on the cell (Levin, 2005), we predicted enhanced synergy between clofazimine and caspofungin at elevated temperature. Growth of both *S. cerevisiae* and *C. albicans* at 39°C exacerbated the synergy observed between caspofungin and clofazimine (Figure 6D). Perturbation of the cell membrane and/or cell wall can often be rescued by osmotic stabilization. In both *S. cerevisiae* and *C. albicans*, the addition of the osmotic stabilizer sorbitol abrogated synergy observed between caspofungin and clofazimine (Figure S5A), suggesting osmotic support reduces the effects of membrane stress caused by clofazimine. Checkerboard as-

### Figure 5. Genome-wide Chemical-Genetic Interactions for Clofazimine

(A) Sensitivity of heterozygous essential deletion strains (gray circles) and homozygous deletion strains (blue circles) to clofazimine as assessed by HIP and HOP. Data represent the average Z score for two biological replicates. Those haploid deletion strains that have a Z score more significant than three SDs below the mean are highlighted in red. No heterozygous deletion strains were identified with a Z score less than three SDs below the mean. See also Table S6.

(B) Gene Ontology (GO) Biological Process terms were generated for those deletion mutants that were at least two SDs more sensitive to clofazimine than the mean population. p values were calculated using PANTHER Overrepresentation Test via GO Ontology Database. See also Figure S4.

says with clofazimine and the membrane targeting antifungal amphotericin B or the ergosterol biosynthesis inhibitor terbinafine also unveiled enhanced efficacy of the drug combination in all four species tested (Figure S5B).

Cells that experience membrane stress activate the Pkc1 signaling pathway, as measured by phosphorylation of the terminal MAP kinase Slt2 (Levin, 2005). We treated *S. cerevisiae* with clofazimine and monitored Slt2 phosphorylation. Exposure to clofazimine increased phosphorylation of Slt2 relative to total levels (Figure 6E). The phosphorylation

of Slt2 induced by clofazimine occurred regardless of whether caspofungin, another activator of Pkc1 signaling, was present. Pkc1 is an essential protein in *S. cerevisiae*; therefore, we monitored the growth of the *PKC1* heterozygous deletion mutant, as well as growth of homozygous deletion mutants elsewhere in the pathway in order to determine whether this signaling cascade was required for tolerance to clofazimine. All mutants displayed increased sensitivity to clofazimine compared to a wild-type control strain ( $p < 0.001$ , ANOVA, Bonferroni's multiple comparison test; Figure 6F), except for deletion of *SWI4*. We also tested a *pkc1Δ/pkc1Δ* homozygous deletion strain in *C. albicans*, where Pkc1 is not essential but is required for tolerance to cell membrane stress (LaFayette et al., 2010). Deletion of *PKC1* abolished growth of *C. albicans* in the presence of clofazimine and complementation of the *pkc1* mutation in a *pkc1/pkc1 + PKC1* strain restored growth back to wild-type levels ( $p < 0.001$ ; Figure 6F). Taken together, these data suggest that clofazimine elicits a cell membrane stress response in both *C. albicans* and *S. cerevisiae*, which activates the Pkc1 signaling pathway.

The chemical-genetic profile for clofazimine suggested it could be generating reactive oxygen species leading to an oxidative stress against *S. cerevisiae*. Similar mechanisms have been reported in *Mycobacterium smegmatis* such that growth of the bacteria in the presence of antioxidants blocks

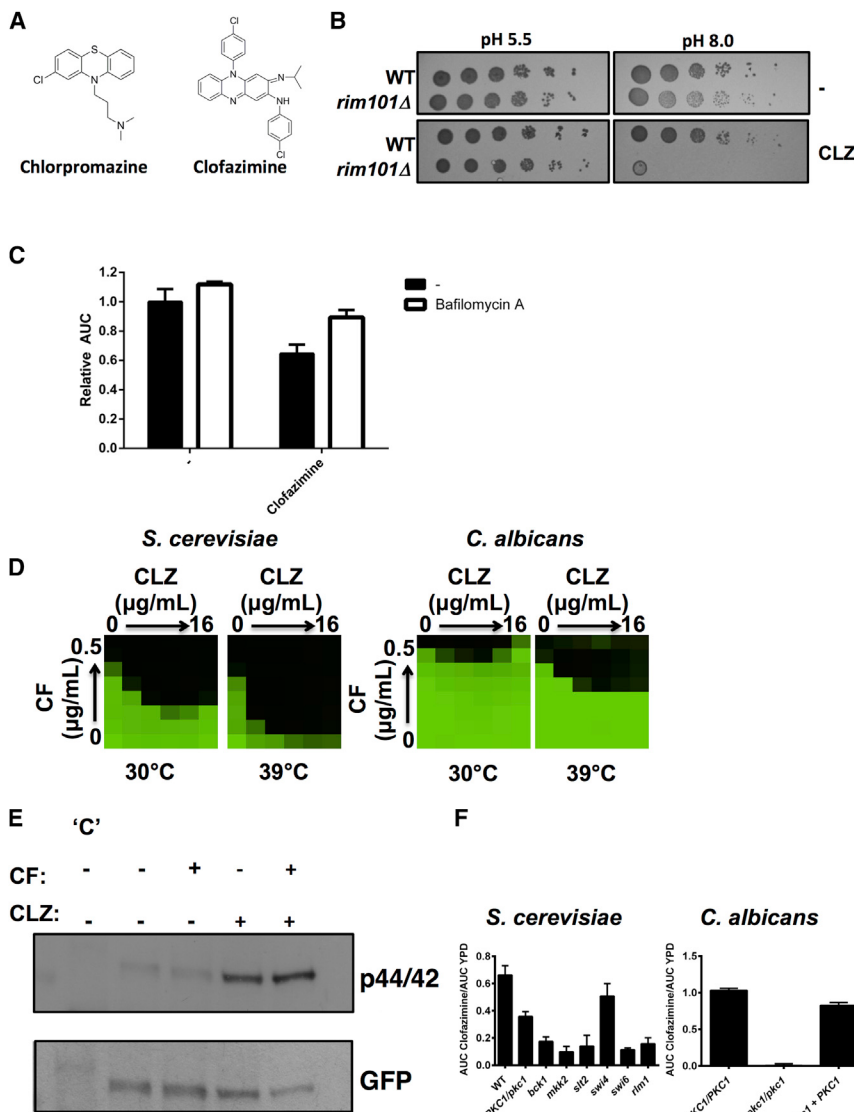


**Figure 6. Clofazimine Acts as a Membrane Perturbing Agent in Fungi**

(A) Structures of the membrane perturbing agents chlorpromazine and clofazimine.

(B) Acidic pH blocks the toxic effects observed by clofazimine (CLZ). Cells were spotted in 5-fold dilutions from  $\sim 1 \times 10^6$  cells/ml onto solid buffered YPD medium with 32  $\mu\text{g}/\text{ml}$  of clofazimine as indicated.

(C) Clofazimine-induced toxicity is rescued by baflomycin A. Growth of *S. cerevisiae* was monitored by measuring the OD<sub>600</sub> for 36 hr. Area under the curve (AUC) was calculated and normalized to solvent treated control. Data are means  $\pm$  SD of triplicate experiments.

(D) Elevated temperature exacerbates the synergy observed between CF and CLZ. Checkerboards were performed and analyzed as in Figure 4.

(E) Treatment of *S. cerevisiae* with CLZ activates Pkc1 signaling as measured by Slt2 phosphorylation. A strain of *S. cerevisiae* harboring an allele of *SLT2* C-terminally GFP tagged was treated with CLZ or CF as indicated. Total protein was resolved by SDS-PAGE, and blots were hybridized with an  $\alpha$ -phospho p44/42 MAPK antibody to monitor phosphorylated Slt2 levels and an  $\alpha$ -GFP antibody to monitor total Slt2 levels. "C" indicates untagged control strain.

(F) Deletion mutants in *S. cerevisiae* or *C. albicans* were grown in the absence and presence of 128  $\mu\text{g}/\text{ml}$  CLZ for 26 hr. Area under the curve (AUC) was calculated in the presence and absence of drug. Data are means  $\pm$  SD of quadruplicates. See also Figure S5.

the toxic effects induced by clofazimine (Yano et al., 2011). To address this possibility, we sought to determine whether we could abolish the synergy observed between clofazimine and caspofungin upon addition of antioxidants; however, the synergy observed between compounds was maintained in the presence of structurally diverse antioxidants  $\alpha$ -tocopherol or *N*-acetyl-L-cysteine (Figure S5C). Thus, we propose that the primary mode of action of clofazimine in yeast is through membrane perturbation, not through the generation of oxidative stress.

#### Clofazimine Potentiates Antifungals in Diverse Fungal Pathogens

To assess the clinical relevance of clofazimine as a combination agent against fungal pathogens, we assessed its ability to potentiate caspofungin against diverse *Candida* species. MIC assays were performed using a gradient of caspofungin without and with a fixed dose of clofazimine. The addition of clofazimine

reduced the caspofungin MIC for all *Candida* species tested (Figure 7A). Clofazimine also reduced the caspofungin MIC for three clinical isolates of *C. albicans* although to a lesser extent (Figure 7A). Next, we assessed whether clofazimine could be used as a combination agent to treat *A. fumigatus* infections, a leading fungal pathogen of humans.

Checkerboard assays were performed with a gradient of caspofungin and clofazimine, and growth was monitored by both optical density and by microscopy due to the filamentous nature of the fungus. Clofazimine potentiated the activity of caspofungin against *A. fumigatus* (Figure 7B), and dramatic reductions in *A. fumigatus* hyphal growth and alterations in hyphal morphology were observed with the drug combination relative to individual drug treatments (Figure 7C). Similar effects were seen with the azole posaconazole in combination with clofazimine (Figure 7C). Clofazimine thus enhances the efficacy of the azole and echinocandin antifungal classes in *A. fumigatus*.

We explored the therapeutic potential of clofazimine in combination with caspofungin against *C. albicans* in an *in vivo* model of infection. We used a tractable invertebrate model, the greater wax moth *G. mellonella*, to study candidiasis *in vivo*. We injected each larvae with  $10^5$  cells of a clinical isolate of *C. albicans* and monitored survival every 24 hr. Injection of larvae with

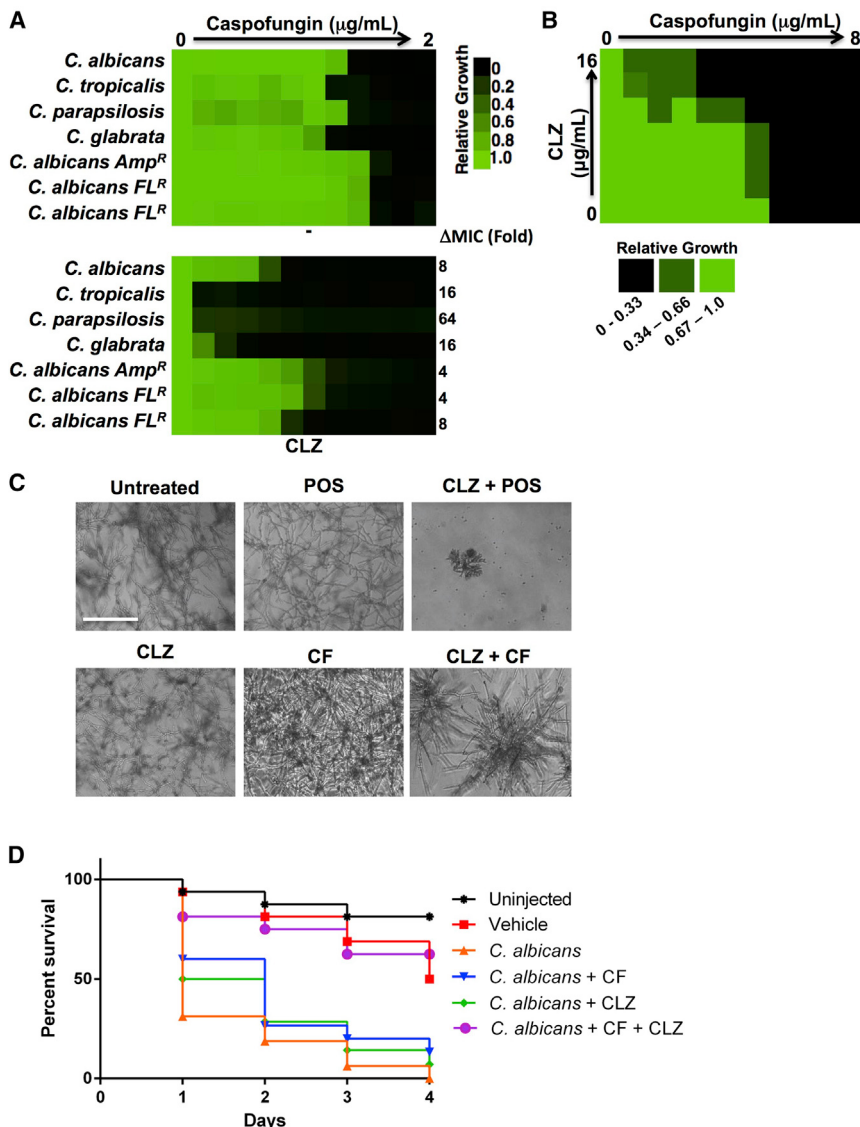


**Figure 7. Clofazimine Potentiates Antifungals in Evolutionary Diverse Fungal Pathogens and in an In Vivo Model of Infection**

(A) Caspofungin (CF) MIC assays were conducted against multiple non *albicans* *Candida* species and against clinical isolates of *C. albicans* that are known to be resistant to indicated antifungals. MICs were conducted in the absence (-) or presence of a fixed concentration of clofazimine (CLZ). Changes in MIC in the presence of CLZ are indicated. Data were analyzed as described in Figure 4.

(B) Checkerboard analysis was conducted with a gradient of caspofungin and a gradient of CLZ in *A. fumigatus*. Growth was quantified and analyzed as described in Figure 4. See scale bar.

(C) Images show *A. fumigatus* incubated with CLZ (16  $\mu\text{g/ml}$ ) in combination with posaconazole (POS, 0.0625  $\mu\text{g/ml}$ ) or CF (0.125  $\mu\text{g/ml}$ ). Images were acquired at a 20 $\times$  magnification. Scale bar, 100  $\mu\text{m}$ .

(D) CLZ potentiates CF in a *G. mellonella* host-model system. Sixteen larvae per treatment group were infected with  $10^5$  cells of a clinical isolate of *C. albicans*. Larvae were treated with CF (0.01 mg/kg), CLZ (15 mg/kg), or a combination once following infection and were scored daily for viability. p values generated by log-rank (Mantel-Cox) test. See also Figure S6.

*C. albicans* caused ~60% death within 1 day and 100% death after 4 days (Figure 7D). Treatment of injected larvae with low doses of individual drug treatments had no effect on survival. Strikingly, a combination treatment rescued growth of *G. mellonella* to a similar level as that observed in the vehicle control ( $p < 0.001$ , log-rank test). Thus, combination therapy with clofazimine and caspofungin rescues lethal *C. albicans* infections in an in vivo invertebrate model.

## DISCUSSION

There is an urgent unmet clinical need to identify new leads to treat systemic fungal infections. To address this need, we optimized a systematic approach to uncover compounds previously unknown to synergize with antifungal agents by combining sub-lethal concentrations of six known antifungals with ~3,600 bioactive compounds, including hundreds of off-patent drugs.

By exploring these interactions in evolutionary diverse fungal species, we unveiled a broad spectrum of chemical-chemical interactions, which we termed the ACM. This dramatically expands the spectrum of previously known antifungal potentiators using molecules that are not employed as antifungals per se but are small molecules previously approved for other indications with well-characterized pharmacokinetic properties or with other bioactivities. Within this rich dataset, we identified a subset of drug combinations

that were active against a fluconazole-resistant *C. albicans* clinical isolate, suggesting additional drug combinations in the ACM are likely active against drug-resistant fungal species. Finally, we determined the mechanism of action of clofazimine, an antimycobacterial compound for which antifungal activity had not previously been described, but which we showed has broad therapeutic potential against fungi. Thus, the ACM dataset is an invaluable resource for research and clinical communities to investigate combination therapeutics with favorable efficacy against harmful fungal pathogens.

Few antifungal potentiators are conserved across the different fungal species investigated in the ACM. Little cross-species overlap was also observed in a previous study that specifically looked for potentiators of fluconazole (Spitzer et al., 2011). The highly specific effects drug combinations have on distinct species can be attributed to multiple factors. Hundreds of millions of years of evolution have altered the way different species

respond to stress induced by small molecules. Fluconazole alone elicits distinct responses to cope with the drug-induced stress in different fungal species. *S. cerevisiae* enhances sterol import, and *C. glabrata* enhances fluconazole export to tolerate azole exposure (Kuo et al., 2010). Further, in *S. cerevisiae* and *C. albicans* distinct cellular circuitries involving the Pkc1 and calcineurin signal transduction cascades are involved in response to fluconazole (LaFayette et al., 2010). Recently, a large-scale chemogenomic atlas was generated for *C. neoformans* and was compared to similar chemical-genetic profiles in *S. cerevisiae* (Brown et al., 2014). The chemical-genetic interactions identified between fungal pathogen and model yeast were largely distinct, even among orthologous genes (Brown et al., 2014). Our work further reinforces the importance of pathogen-focused investigation and is the first dataset of this magnitude that explores combinatorial agents in two evolutionary diverse fungal pathogens.

A key public health concern is the rapid development of resistance many fungal pathogens, most notably *C. albicans*, have to current antifungal treatments (Centers for Disease Control and Prevention, 2013). In a fluconazole-resistant isolate of *C. albicans*, we observed potent synergistic interactions between fluconazole and chlorhexidine, hypocrellin A, or tomatidine. There are numerous mutations readily acquired in clinical settings that confer fluconazole resistance in *C. albicans* including, but not limited to, mutations in the azole target Erg11 and mutations involving upregulation of drug efflux pumps (Shapiro et al., 2011). The nature of the resistance mechanism often dictates whether particular drug combinations will be efficacious. Mutations in *TAC1*, a transcriptional activator of the CDR drug efflux pumps, maintain resistance to fluconazole in the presence of calcineurin or Hsp90 inhibitors (Hill et al., 2015). The clinical isolate used in our studies harbored several nonsynonymous substitutions in *TAC1*, including a hyperactive mutation, Tac1<sup>T225A</sup>, capable of conferring fluconazole resistance (Coste et al., 2007). We also identified a nonsynonymous mutation in *ERG11* located in a “hot-spot” region predisposed to mutations that confer fluconazole resistance (Marichal et al., 1999). Although additional work remains to assess the impact each of these mutations has in conferring fluconazole resistance, it remains intriguing that chlorhexidine, hypocrellin A, and tomatidine are able to potentiate fluconazole in this strain and warrants further investigation into the manner by which they do so.

We selected clofazimine for mechanistic studies due to its broad, yet unreported, activity against diverse fungal species. A genome-wide chemical-genetic profile combined with cell biological phenotypes suggests clofazimine diffuses across the plasma membrane and intercalates into the cytosolic side of the lipid bilayer, which manifests in a cell membrane stress. This is supported by studies in bacteria that have shown clofazimine is a membrane-destabilizing agent, dismantling membrane architecture directly and by interacting with lysophospholipids (Cholo et al., 2012). Recently, derivatives of amphotericin B were generated that displayed high selectivity to pathogen-specific lipids in vitro and potent efficacy in mouse models of fungal pathogenesis (Davis et al., 2015). These compounds strongly evaded the emergence of resistance, likely because

ergosterol serves as a central molecular node in a myriad of essential cellular processes (Davis et al., 2015). As our work implicates membrane lipids as a target of clofazimine, we postulate this compound could similarly impede resistance development. Clofazimine dramatically improved the efficacy of caspofungin in non-albicans *Candida*. Notably, the incidence of candidemia due to other *Candida* species such as *C. parapsilosis* and *C. glabrata* has increased significantly over the last 2 decades (Cleveland et al., 2012). Alarmingly, resistance to fluconazole and echinocandins is more common in non-albicans *Candida* compared with *C. albicans* isolates (Cleveland et al., 2012), necessitating the development of new treatment strategies in these species. As predicted by our in vitro data, combination therapy with clofazimine and caspofungin rescues a lethal *C. albicans* infection in the invertebrate host *G. mellonella*. However, preliminary experiments in a mouse model of disseminated *C. albicans* infection did not support our in vitro data (Figure S6), presumably due to unfavorable pharmacokinetic properties against the drug combinations in this more complex model system. Additional experiments using altered routes of administration and/or infections with other fungal pathogens may still unveil conditions for the use of clofazimine as a treatment for fungal infections.

The generation of the ACM charted a new realm of chemical space, which has been and will continue to be exploited for both fundamental biological research and as an approach to accelerate drug development. We know more efficacious and specific intervention for the treatment of infectious disease can be achieved through the combinations of bioactive compounds. The challenge that remains for us and other members of the medical mycology community is to identify and explore those combinations whose strong in vitro synergistic interactions can be translated to potent therapies in mammalian models of fungal infections.

## EXPERIMENTAL PROCEDURES

### Ethics Statement

Animals studies were conducted in the Division of Laboratory Animal Resources (DLAR) facilities at Duke University Medical Center (DUMC) in good practice as defined by the United States Animal Welfare Act and in full compliance with the guidelines of the DUMC Institutional Animal Care and Use Committee (IACUC). The vertebrate animal experiments were reviewed and approved by the DUMC IACUC under protocol number A114-14-05.

### Strains and Culture Conditions

Strains are listed in Table S7, and culture conditions are described in the Supplemental Experimental Procedures.

### High-Throughput Screening

The McMaster Bioactives collection was screened at a final concentration of 12.5  $\mu$ M in the presence and absence of 1/4 MIC antifungal. Screens were performed using *C. albicans* (ATCC 90028), *C. neoformans* (H99), *S. cerevisiae* (BY4741), and *S. pombe* (ATCC 38366). Details of screening methods are described in the Supplemental Experimental Procedures. In brief, screens were conducted in duplicate in 384-well flat-bottom microtiter plates (Thermo Scientific) at a final volume of 80  $\mu$ L. For preparation of diluted yeast culture, liquid overnight cultures were diluted to an OD<sub>600</sub> of 0.14, followed by a 1:1,000 dilution in synthetic complete (SC) media. Plates were incubated at 30°C and OD<sub>600</sub> was measured after 48 hr of growth for *S. cerevisiae* and *C. albicans* or 72 hr of growth for *C. neoformans* and *S. pombe*. All data were

normalized for plate- and row/column-specific effects as described previously (Spitzer et al., 2011). Screen hits were those compounds that were three MADs below the diagonal, inhibited growth on their own less than 50%, and resulted in at least 80% growth inhibition in the presence of the antifungal. Chemical-chemical interactions were generated using the program Cytoscape v3.2.1 using a spring embedded algorithm (<http://www.cytoscape.org>).

#### Drug Susceptibility Assays

All compounds were purchased from Sigma Aldrich with the exception of caspofungin (Cancidas) and posaconazole, which were purchased from Merck, and hypocrellin A, which was purchased from Abcam. DMSO (Sigma-Aldrich) was the solvent for all compounds. Drug susceptibility assays were performed as described previously (LaFayette et al., 2010). Details of protocol are described in the *Supplemental Experimental Procedures*. For *A. fumigatus*, drug susceptibility was determined using a 24-well plate assay (Corning). Each well was inoculated with  $10^5$  conidia of *A. fumigatus* Af293. The plates were incubated at 37°C and 5% CO<sub>2</sub> and examined after 24 and 48 hr under an inverted light microscope (Zeiss). Images acquired using Infinity2 camera (Lumenera).

#### Cidality Assays

Viability of cultures after treatment with a gradient of fluconazole in combination with a gradient of ACM compound were tested by spotting 2 µl on YPD plates after yeast cells had been incubated with compound for 48 hr. YPD agar plates were incubated at 30°C for 48 hr prior to imaging.

#### Spotting Assays

Strains were grown to saturation in YPD, and cell concentrations were standardized based on optical density. 5-fold dilutions (from  $\approx 1 \times 10^6$  cells/ml) were spotted onto pH-buffered media with and without clofazimine. Plates were photographed after 2 days in the dark at 30°C.

#### Chemical-Genomic Assays

*S. cerevisiae* deletion collections (MAT $\alpha$  haploid and heterozygous essential deletion strains) were obtained from Research Genetics (Germany). Details of protocol are described in the *Supplemental Experimental Procedures*. In brief, compounds were screened at a concentration that inhibited growth of the pool by ~20% relative to a solvent control. Deletion pools were grown for 24 hr at which point gDNA was extracted using phenol-chloroform extraction methods. Purified gDNA was used to amplify the barcoded tags upstream of the KANMX cassette using various primer combinations (Table S8). PCR products were pooled and sequenced at the Farncombe Metagenomics Facility at McMaster University. p values for Gene Ontology (GO) enrichment were calculated through the Gene Ontology Consortium resource (<http://geneontology.org>) (Gene Ontology, 2015).

#### Immune Blot Analysis

Immunoblotting was conducted as described previously (LaFayette et al., 2010). In brief, a strain of *S. cerevisiae* harboring a GFP epitope tag on Slt2 was grown overnight in YPD at 30°C without and with 10 µg/ml of clofazimine. In the morning, cells were diluted to OD<sub>600</sub> of 0.2 in 125 ml of YPD without or with clofazimine and grown to mid-log (~5 hr) at 30°C. Cultures were split and left untreated or treated with 50 ng/ml of caspofungin for 30 min. Cells were harvested and total protein extracts were prepared as described previously (Robbins et al., 2011). Protein concentrations were determined by Bradford analysis. Samples were separated by 10% SDS-PAGE. Protein was electrotransferred to polyvinylidene fluoride (PVDF) membrane, blocked with 5% BSA in Tris-buffered saline with 0.1% Tween. Blots were hybridized with antibodies against GFP (1:750 dilution, Cell Signaling Technology, 2956P) and phospho-p44/42 MAPK (Thr202/Tyr204) (1:750, Cell Signaling Technology, 9101S).

#### *G. mellonella* Antifungal Assay

Injection of *C. albicans* and antifungal drugs was performed essentially as described (Fuchs et al., 2010). In brief, larvae in the final instar were obtained from Reptilia: Reptile Zoo and Educational Facility. Sixteen larvae (275 ± 25 mg) were used per group. Each injection of 5 µl of fungus, drug, or control

into the hemocoel was performed via a distinct proleg. Drugs were injected after inoculum delivery. Larvae were incubated at 37°C, and the number of dead larvae was scored daily. *C. albicans* inoculum was prepared by growing YPD cultures overnight at 30°C. Cells were washed three times in PBS, densities were determined by hemacytometer count, and dilutions were prepared in PBS. Kill curves were plotted and estimation of differences in survival (log-rank test) analyzed by the Kaplan-Meier method (GraphPad Prism). Killing assays were performed twice using distinct batches of *G. mellonella*.

#### SUPPLEMENTAL INFORMATION

Supplemental Information includes Supplemental Experimental Procedures, six figures, and eight tables and can be found with this article online at <http://dx.doi.org/10.1016/j.celrep.2015.10.018>.

#### AUTHOR CONTRIBUTIONS

Conceptualization, N.R., M.T., and G.D.W.; Methodology, N.R., Y.S.B., J.H., D.C.S., M.T., and G.D.W.; Formal Analysis, N.R., M.S., Investigation, N.R., T.Y., R.P.C., A.K.A., and Y.S.B.; Writing – Original Draft, N.R. and G.D.W.; Writing – Review & Editing, N.R., M.S., J.H., D.C.S., M.T., and G.D.W.; Visualization, N.R., M.S.; Funding Acquisition, M.T and G.D.W.; Resources, J.H.; Supervision, J.H., D.C.S., M.T., and G.D.W.

#### ACKNOWLEDGMENTS

We thank Leah Cowen for strains and Leah Cowen, Troy Ketela, and G.D.W.'s lab members for helpful discussions. N.R. was supported by the Michael G. DeGroote Postdoctoral Fellowship Award and a Canadian Institute for Health Research (CIHR) Fellowship. G.D.W. and M.T. were supported by Canada Research Chairs in Antibiotic Biochemistry and Systems and Synthetic Biology respectively. Research was funded by grants from CIHR (MOP 119572 to M.T. and G.D.W.), the European Research Council (SCG-233457 to M.T.), the NIH (1R01-AI112595 to J.H.) and Wellcome Trust (085178 to M.T.).

Received: August 21, 2015

Revised: September 22, 2015

Accepted: October 6, 2015

Published: November 5, 2015

#### REFERENCES

- Anderson, N., and Borlak, J. (2006). Drug-induced phospholipidosis. *FEBS Lett.* **580**, 5533–5540.
- Anderson, T.M., Clay, M.C., Cioffi, A.G., Diaz, K.A., Hisao, G.S., Tuttle, M.D., Nieuwkoop, A.J., Comellas, G., Maryum, N., Wang, S., et al. (2014). Amphotericin forms an extramembranous and fungicidal sterol sponge. *Nat. Chem. Biol.* **10**, 400–406.
- Blankenship, J.R., Steinbach, W.J., Perfect, J.R., and Heitman, J. (2003). Teaching old drugs new tricks: reincarnating immunosuppressants as anti-fungal drugs. *Curr. Opin. Investig. Drugs* **4**, 192–199.
- Borisy, A.A., Elliott, P.J., Hurst, N.W., Lee, M.S., Lehar, J., Price, E.R., Serbedzija, G., Zimmermann, G.R., Foley, M.A., Stockwell, B.R., and Keith, C.T. (2003). Systematic discovery of multicomponent therapeutics. *Proc. Natl. Acad. Sci. USA* **100**, 7977–7982.
- Brown, G.D., Denning, D.W., Gow, N.A., Levitz, S.M., Netea, M.G., and White, T.C. (2012). Hidden killers: human fungal infections. *Sci. Transl. Med.* **4**, 165rv13.
- Brown, J.C., Nelson, J., VanderSluis, B., Deshpande, R., Butts, A., Kagan, S., Polacheck, I., Krysan, D.J., Myers, C.L., and Madhani, H.D. (2014). Unraveling the biology of a fungal meningitis pathogen using chemical genetics. *Cell* **159**, 1168–1187.
- Butts, A., DiDone, L., Kosekny, K., Baxter, B.K., Chabrier-Rosello, Y., Wellington, M., and Krysan, D.J. (2013). A repurposing approach identifies

- off-patent drugs with fungicidal cryptococcal activity, a common structural chemotype, and pharmacological properties relevant to the treatment of cryptococcosis. *Eukaryot. Cell* 12, 278–287.
- Centers for Disease Control and Prevention (2013). Antibiotic Resistance Threats in the United States, 2013. U.S. Department of Health and Human Services (CDC).
- Cholo, M.C., Steel, H.C., Fourie, P.B., Germishuizen, W.A., and Anderson, R. (2012). Clofazimine: current status and future prospects. *J. Antimicrob. Chemother.* 67, 290–298.
- Cleveland, A.A., Farley, M.M., Harrison, L.H., Stein, B., Hollick, R., Lockhart, S.R., Magill, S.S., Derado, G., Park, B.J., and Chiller, T.M. (2012). Changes in incidence and antifungal drug resistance in candidemia: results from population-based laboratory surveillance in Atlanta and Baltimore, 2008–2011. *Clin. Infect. Dis.* 55, 1352–1361.
- Costanzo, M., Baryshnikova, A., Bellay, J., Kim, Y., Spear, E.D., Sevier, C.S., Ding, H., Koh, J.L., Toufighi, K., Mostafavi, S., et al. (2010). The genetic landscape of a cell. *Science* 327, 425–431.
- Coste, A., Selmecki, A., Forche, A., Diogo, D., Bougnoux, M.E., d'Enfert, C., Berman, J., and Sanglard, D. (2007). Genotypic evolution of azole resistance mechanisms in sequential *Candida albicans* isolates. *Eukaryot. Cell* 6, 1889–1904.
- Cowen, L.E., Singh, S.D., Köhler, J.R., Collins, C., Zaas, A.K., Schell, W.A., Aziz, H., Mylonakis, E., Perfect, J.R., Whitesell, L., and Lindquist, S. (2009). Harnessing Hsp90 function as a powerful, broadly effective therapeutic strategy for fungal infectious disease. *Proc. Natl. Acad. Sci. USA* 106, 2818–2823.
- Davis, S.A., Vincent, B.M., Endo, M.M., Whitesell, L., Marchillo, K., Andes, D.R., Lindquist, S., and Burke, M.D. (2015). Nontoxic antimicrobials that evade drug resistance. *Nat. Chem. Biol.* 11, 481–487.
- Day, J.N., Chau, T.T., Wolbers, M., Mai, P.P., Dung, N.T., Mai, N.H., Phu, N.H., Nghia, H.D., Phong, N.D., Thai, C.Q., et al. (2013). Combination antifungal therapy for cryptococcal meningitis. *N. Engl. J. Med.* 368, 1291–1302.
- De Filippi, L., Fournier, M., Cameroni, E., Linder, P., De Virgilio, C., Foti, M., and Deloche, O. (2007). Membrane stress is coupled to a rapid translational control of gene expression in chlorpromazine-treated cells. *Curr. Genet.* 52, 171–185.
- Denning, D.W., and Bromley, M.J. (2015). Infectious Disease. How to bolster the antifungal pipeline. *Science* 347, 1414–1416.
- Fuchs, B.B., O'Brien, E., Khoury, J.B., and Mylonakis, E. (2010). Methods for using *Galleria mellonella* as a model host to study fungal pathogenesis. *Virulence* 1, 475–482.
- Gene Ontology, C.; Gene Ontology Consortium (2015). Gene Ontology Consortium: going forward. *Nucleic Acids Res.* 43, D1049–D1056.
- Giaever, G., Flaherty, P., Kumm, J., Proctor, M., Nislow, C., Jaramillo, D.F., Chu, A.M., Jordan, M.I., Arkin, A.P., and Davis, R.W. (2004). Chemogenomic profiling: identifying the functional interactions of small molecules in yeast. *Proc. Natl. Acad. Sci. USA* 101, 793–798.
- Gilbert, P., and Moore, L.E. (2005). Cationic antiseptics: diversity of action under a common epithet. *J. Appl. Microbiol.* 99, 703–715.
- Hill, J.A., O'Meara, T.R., and Cowen, L.E. (2015). Fitness Trade-Offs Associated with the Evolution of Resistance to Antifungal Drug Combinations. *Cell Rep.* 10, 809–819.
- Kuo, D., Tan, K., Zinman, G., Ravasi, T., Bar-Joseph, Z., and Ideker, T. (2010). Evolutionary divergence in the fungal response to fluconazole revealed by soft clustering. *Genome Biol.* 11, R77.
- LaFayette, S.L., Collins, C., Zaas, A.K., Schell, W.A., Betancourt-Quiroz, M., Gunatilaka, A.A., Perfect, J.R., and Cowen, L.E. (2010). PKC signaling regulates drug resistance of the fungal pathogen *Candida albicans* via circuitry comprised of *Mkc1*, calcineurin, and *Hsp90*. *PLoS Pathog.* 6, e1001069.
- Lee, A.Y., St Onge, R.P., Proctor, M.J., Wallace, I.M., Nile, A.H., Spagnuolo, P.A., Jitkova, Y., Gronda, M., Wu, Y., Kim, M.K., et al. (2014). Mapping the cellular response to small molecules using chemogenomic fitness signatures. *Science* 344, 208–211.
- Levin, D.E. (2005). Cell wall integrity signaling in *Saccharomyces cerevisiae*. *Microbiol. Mol. Biol. Rev.* 69, 262–291.
- Marichal, P., Koymans, L., Willemse, S., Bellens, D., Verhasselt, P., Luyten, W., Borgers, M., Ramaekers, F.C., Odds, F.C., and Bossche, H.V. (1999). Contribution of mutations in the cytochrome P450 14alpha-demethylase (*Erg11p*, *Cyp51p*) to azole resistance in *Candida albicans*. *Microbiology* 145, 2701–2713.
- Odds, F.C. (2003). Synergy, antagonism, and what the chequerboard puts between them. *J. Antimicrob. Chemother.* 52, 1.
- Ostrosky-Zeichner, L., Casadevall, A., Galgiani, J.N., Odds, F.C., and Rex, J.H. (2010). An insight into the antifungal pipeline: selected new molecules and beyond. *Nat. Rev. Drug Discov.* 9, 719–727.
- Pierce, S.E., Fung, E.L., Jaramillo, D.F., Chu, A.M., Davis, R.W., Nislow, C., and Giaever, G. (2006). A unique and universal molecular barcode array. *Nat. Methods* 3, 601–603.
- Robbins, N., Uppuluri, P., Nett, J., Rajendran, R., Ramage, G., Lopez-Ribot, J.L., Andes, D., and Cowen, L.E. (2011). Hsp90 governs dispersion and drug resistance of fungal biofilms. *PLoS Pathog.* 7, e1002257.
- Shapiro, R.S., Robbins, N., and Cowen, L.E. (2011). Regulatory circuitry governing fungal development, drug resistance, and disease. *Microbiol. Mol. Biol. Rev.* 75, 213–267.
- Sharom, J.R., Bellows, D.S., and Tyers, M. (2004). From large networks to small molecules. *Curr. Opin. Chem. Biol.* 8, 81–90.
- Simons, V., Morrissey, J.P., Latijnhouwers, M., Csukai, M., Cleaver, A., Yarrow, C., and Osbourn, A. (2006). Dual effects of plant steroid alkaloids on *Saccharomyces cerevisiae*. *Antimicrob. Agents Chemother.* 50, 2732–2740.
- Spitzer, M., Griffiths, E., Blakely, K.M., Wildenhain, J., Ejim, L., Rossi, L., De Pascale, G., Curak, J., Brown, E., Tyers, M., and Wright, G.D. (2011). Cross-species discovery of syncretic drug combinations that potentiate the anti-fungal fluconazole. *Mol. Syst. Biol.* 7, 499.
- Wilson, L.S., Reyes, C.M., Stolpman, M., Speckman, J., Allen, K., and Beney, J. (2002). The direct cost and incidence of systemic fungal infections. *Value Health* 5, 26–34.
- Yano, T., Kassovska-Bratinova, S., Teh, J.S., Winkler, J., Sullivan, K., Isaacs, A., Schechter, N.M., and Rubin, H. (2011). Reduction of clofazimine by mycobacterial type 2 NADH:quinone oxidoreductase: a pathway for the generation of bactericidal levels of reactive oxygen species. *J. Biol. Chem.* 286, 10276–10287.
- Zimmermann, G.R., Lehár, J., and Keith, C.T. (2007). Multi-target therapeutics: when the whole is greater than the sum of the parts. *Drug Discov. Today* 12, 34–42.

**Cell Reports**

**Supplemental Information**

**An Antifungal Combination Matrix Identifies  
a Rich Pool of Adjuvant Molecules that Enhance  
Drug Activity against Diverse Fungal Pathogens**

**Nicole Robbins, Michaela Spitzer, Tennison Yu, Robert P. Cerone, Anna K. Averette,  
Yong-Sun Bahn, Joseph Heitman, Donald C. Sheppard, Mike Tyers, and Gerard D.  
Wright**

Figure S1

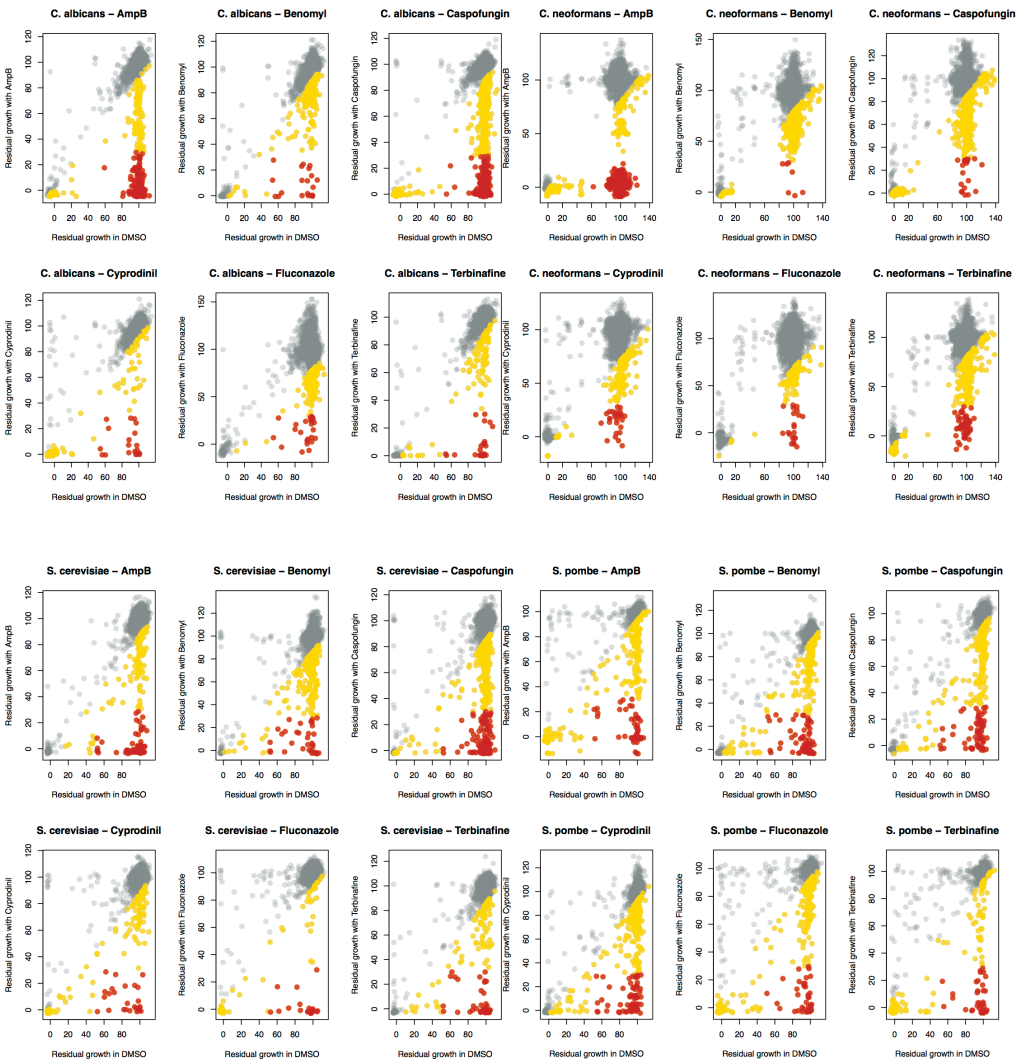


Figure S2

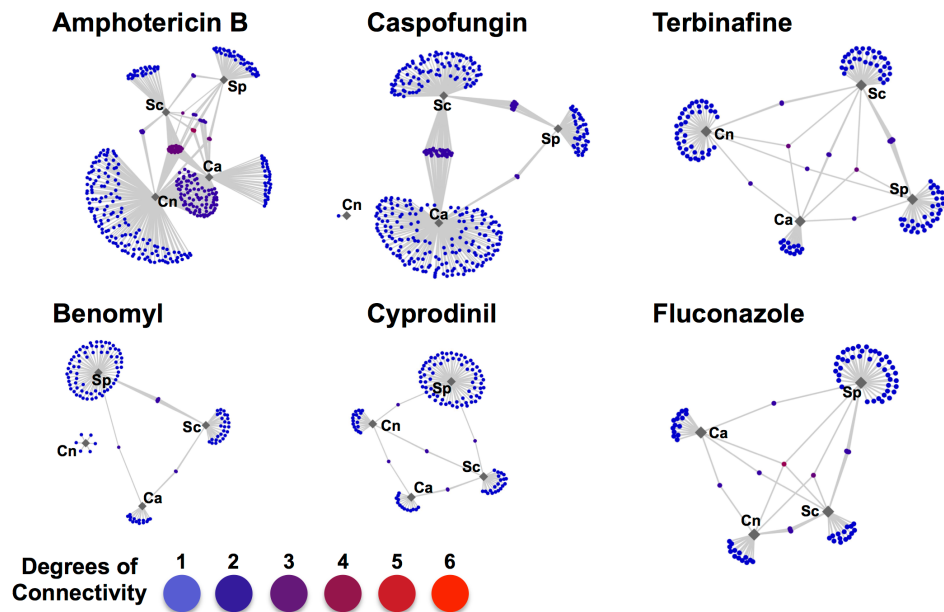


Figure S3

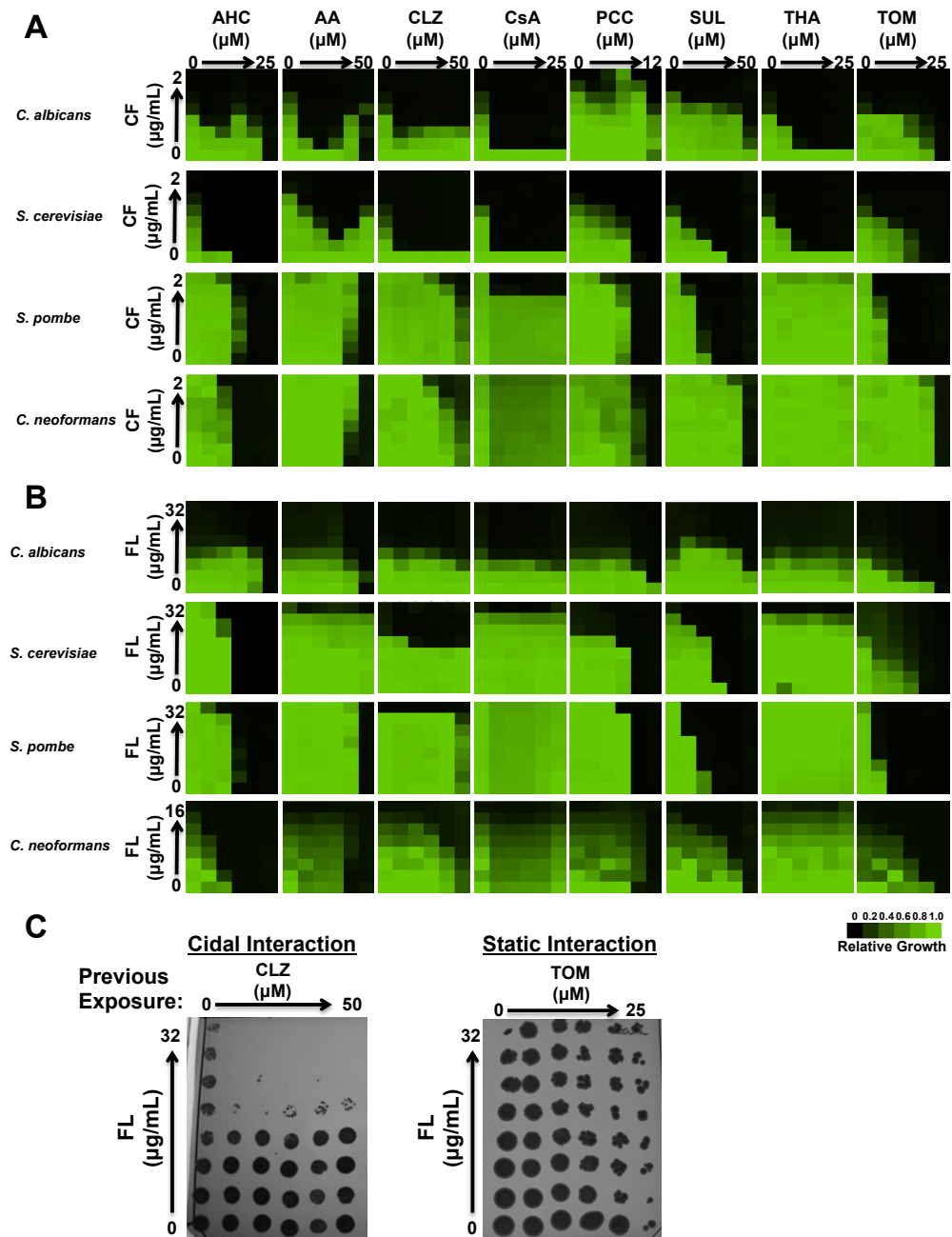


Figure S4

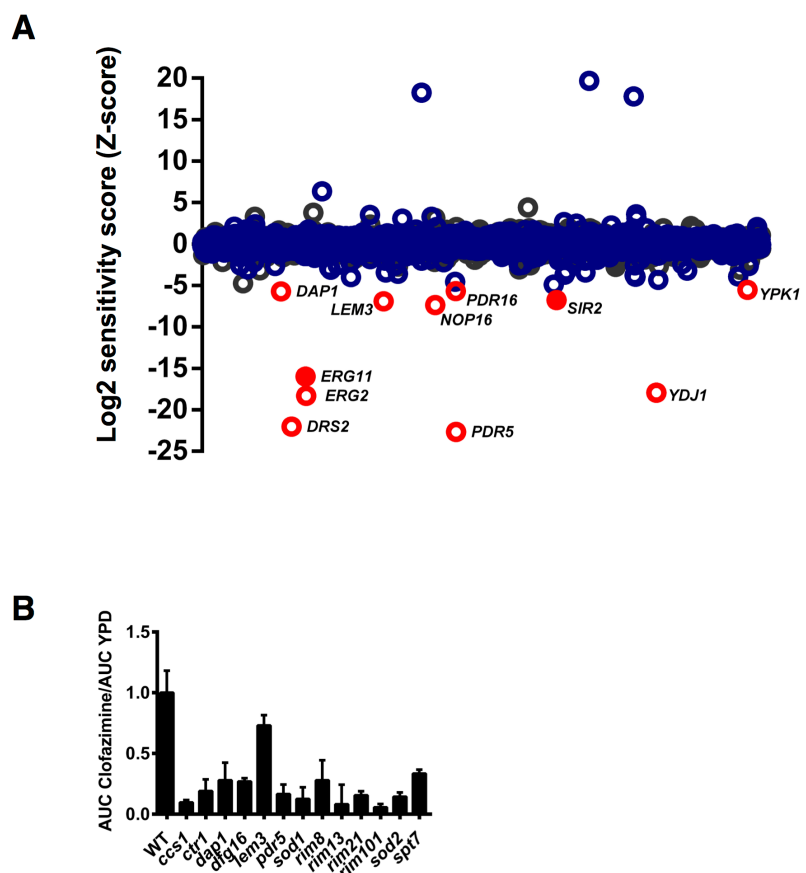


Figure S5

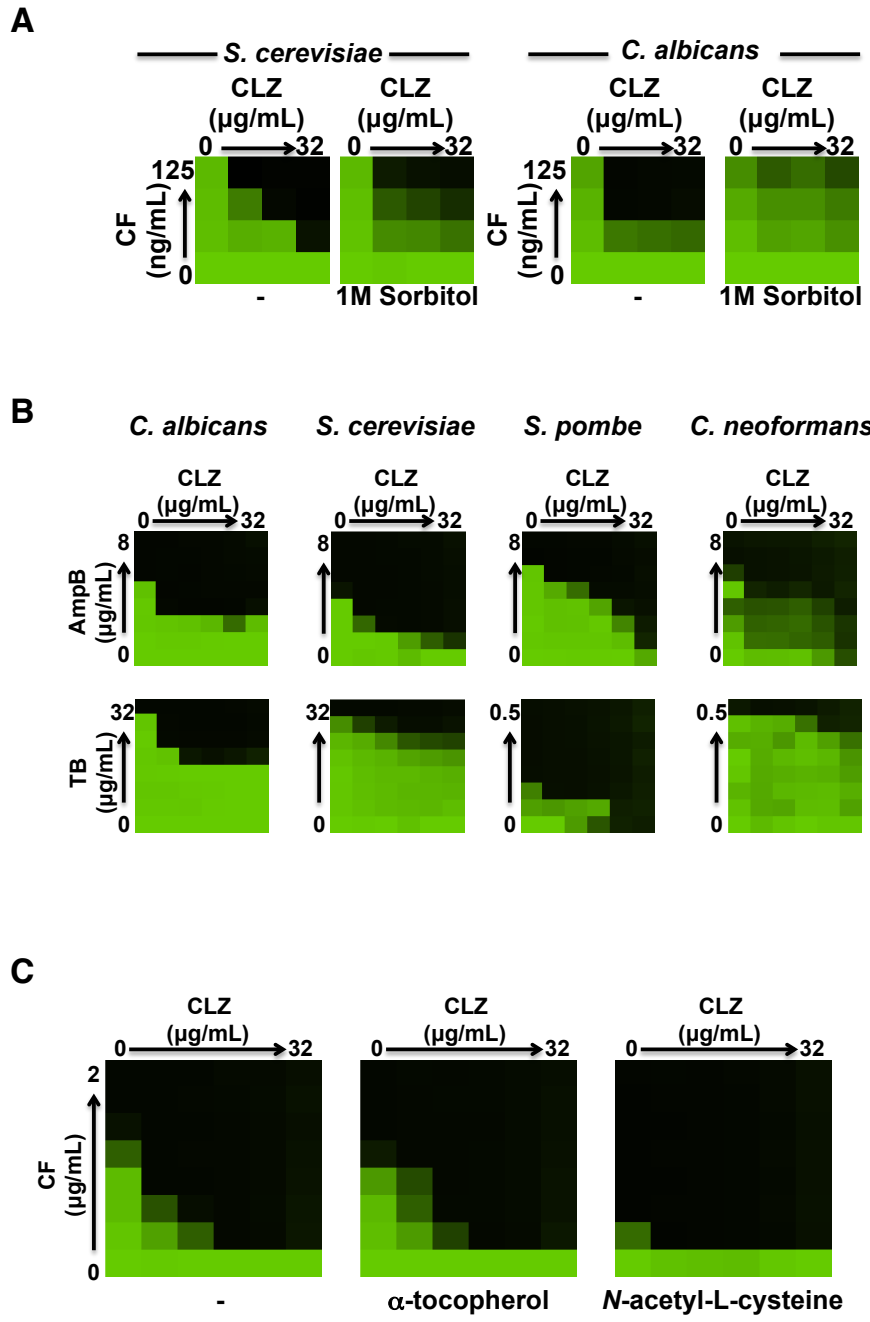
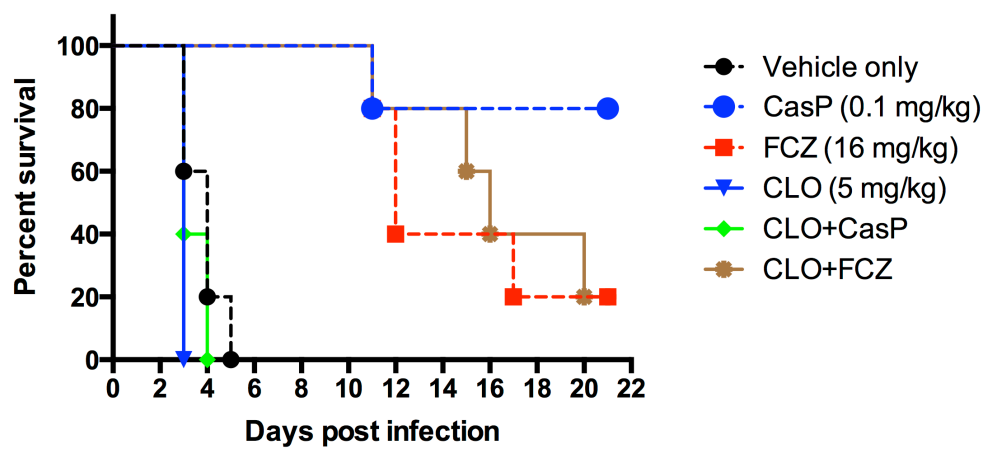


Figure S6



## SUPPLEMENTAL FIGURE LEGENDS

**Figure S1. Primary screening data for bioactive compounds that potentiate antifungals in four fungal species.** The scatterplots shows the normalized residual growth of *C. albicans* (top left), *C. neoformans* (top right), *S. cerevisiae* (bottom left), and *S. pombe* (bottom right) for each compound in the absence (x axis) and presence of antifungal (y axis). Those compounds that are 3 MADs below the diagonal were colored yellow. Compounds that were 3 MADs below the diagonal, inhibited growth less than 50% without antifungal, and inhibited growth greater than 80% with antifungal are colored red. Red compounds were classified as hits and were used for comparative analysis. Related to Figure 1 and Figure 2.

**Figure S2. Chemical-species interaction networks.** Chemical-species networks are generated for each individual antifungal. Compounds that potentiated an antifungal are depicted as circles and are connected by edges to the species in which synergy was observed. Each circle is color-coded to reflect its degree of connectivity (frequency of occurrence in the screens). Species in which the screen was conducted are shown as gray diamonds. (*C. albicans* (Ca), *C. neoformans* (Cn), *S. cerevisiae* (Sc) or *S. pombe* (Sp)). Related to Figure 1 and Figure 2.

**Figure S3. ACM hit validation and characterization. A-B)** Checkerboard assays confirm drug interactions between those compounds identified as hits during screening and caspofungin (CF) (A) or fluconazole (FL) (B). Two-fold serial dilutions of CF or FL were combined with two-fold dilutions of the following compounds: Amiodarone Hydrochloride (AHC), Asiatic Acid (AA), Clofazimine (CLZ), Cyclosporin A (CsA), Palmitoyl-DL-Carnitine Chloride (PCC), Suloctidil (SUL), Thapsigargin (THA), and

Tomatidine (TOM). Growth was measured by OD<sub>600</sub> and data was quantitatively displayed with color using Treeview (see color bar). **C)** Examples of cidal and static drug interactions. Checkerboard assays with two-fold dilutions of FL in combination with CLZ or TOM in *C. albicans* were performed in SC and incubated for 48 hours at 30°C. Cells from the checkerboard assays were spotted onto YPD medium and incubated at 30°C for 48 hours before plates were photographed. Related to Figure 3 and Table S5.

**Figure S4. Genome-wide chemical-genetic interactions for fluconazole and validation of clofazimine sensitive mutants.** **A)** Sensitivity of heterozygous essential deletion strains (gray circles) and homozygous deletion strains (blue circles) to clofazimine as assessed by haploinsuffucency (HIP) and homozygous deletion profiling (HOP). Those deletion strains that have a Z-score more significant than three standard-deviations below the mean are highlighted in red, filled circles represent heterozygous strains and open circles represent homozygous strains. *ERG11*, the known target of fluconazole, was the most sensitive heterozygous deletion strain. The fluconazole exporter *PDR5*, as well as other genes known to be sensitive to fluconazole were identified by HOP analysis. **B)** Deletion strains identified in the HIP-HOP analysis were confirmed to be sensitive to CLZ by growth curve analysis. Individual mutants were grown in the absence and presence of CLZ over 48 hours and the area under the curve (AUC) was calculated. Data are means  $\pm$  standard deviation of triplicates. Related to Figure 5.

**Figure S5. Clofazimine potentiates antifungals in yeast due to perturbation of membranes, not through the generation of oxidative stress.** **A)** Two-fold serial dilutions of caspofungin (CF) were combined with two-fold dilutions of clofazimine

(CLZ) in the absence or presence of 1M sorbitol in SC media. Growth was measured by OD<sub>600</sub> and data was quantitatively displayed with color using Treeview (see color bar). **B)** Two-fold serial dilutions of amphotericin B (AmpB) or terbinafine (TB) were combined with two-fold dilutions of clofazimine (CLZ). Growth was analyzed as in part A. **C)** Two-fold serial dilutions of caspofungin (CF) were combined with two-fold dilutions of CLZ in the absence and presence of antioxidants  $\alpha$ -tocopherol (12.5 $\mu$ g/mL) or *N*-acetyl-L-cysteine (5mM). Data was analyzed as described in part A. Related to Figure 6.

**Figure S6. Clofazimine does not potentiate antifungals in a mammalian model of fungal infection.** CD1 mice were infected with an inoculum of 200  $\mu$ L of  $1 \times 10^6$  CFU/mL of SC5314. Fluconazole (16 mg/kg) and caspofungin (0.1 mg/kg) were administered i.p. and clofazimine (5 mg/kg) was administered by oral gavage. Drugs were given 4 h, 24 h, 48 h, and 72 h post-infection. Viability was scored daily. Related to Figure 7.

**Table S1.**  $\frac{1}{4}$  Minimum Inhibitory Concentration (MIC) of antifungals against different fungal species used for the generation of the ACM. Related to Figure 1.

Compound	<i>C. albicans</i> MIC ( $\mu\text{g/mL}$ )	<i>C. neoformans</i> MIC ( $\mu\text{g/mL}$ )	<i>S. cerevisiae</i> MIC ( $\mu\text{g/mL}$ )	<i>S. pombe</i> MIC ( $\mu\text{g/mL}$ )
Amphotericin B	0.25	1	0.25	0.25
Benomyl	8	2	2	1
Caspofungin	0.13	2*	0.13	0.5
Cyprodinil	16	16	8	2
Fluconazole	0.5	8	8	64
Terbinafine	4	1	16	0.02

\* Since we were unable to calculate a MIC for caspofungin against *C. neoformans* we used a concentration of 2  $\mu\text{g/mL}$  for the primary screen.

**Table S2. Normalized Primary Screening Data.** Related to Figure 1 and Figure 2.

**Table S3. Compounds Identified as Antifungal Potentiators in the Antifungal Combination Matrix.** Related to Figure 1 and Figure 2.

**Table S4. Compounds Identified in the ACM that Potentiated Indicated Antifungal.**  
Related to Figure 3.

<u>Compound</u>	<u>Therapeutic Use</u>	<u>Screen Identified (Species: Antifungal)</u>
Amiodarone Hydrochloride	<ul style="list-style-type: none"> <li>• <math>\text{Na}^+/\text{K}^+</math> channel blocker</li> <li>• Antiarrhythmic</li> </ul>	<i>C. albicans</i> : AmpB, CF <i>C. neoformans</i> : AmpB, FL <i>S. cerevisiae</i> : AmpB, CF, FL
Asiatic Acid	<ul style="list-style-type: none"> <li>• Anticancer</li> </ul>	<i>C. albicans</i> : AmpB, CF, FL <i>C. neoformans</i> : AmpB <i>S. cerevisiae</i> : AmpB, CF <i>S. pombe</i> : AmpB
Clofazimine	<ul style="list-style-type: none"> <li>• Antileprosy agent</li> <li>• Antimycobacterial agent</li> </ul>	<i>C. albicans</i> : AmpB, CF, TB <i>C. neoformans</i> : AmpB
Cyclosporin A	<ul style="list-style-type: none"> <li>• Immunosuppressant</li> <li>• Calcineurin inhibitor</li> </ul>	<i>C. albicans</i> : AmpB, CF, TB <i>C. neoformans</i> : AmpB, Cyp, FL, TB <i>S. cerevisiae</i> : AmpB, CF, TB
Palmitoyl-DL-Carnitine Chloride	<ul style="list-style-type: none"> <li>• Protein Kinase C inhibitor</li> </ul>	<i>S. cerevisiae</i> : AmpB, Ben, CF, Cyp, FL, TB
Suloctidil	<ul style="list-style-type: none"> <li>• Vasodilator</li> <li>• Hypocholesterolemic drug</li> </ul>	<i>C. albicans</i> : CF <i>C. neoformans</i> : AmpB, Cyp, FL <i>S. cerevisiae</i> : CF, FL, TB <i>S. pombe</i> : FL, TB
Thapsigargin	<ul style="list-style-type: none"> <li>• Sarco-endoplasmic reticulum <math>\text{Ca}(2+)</math>-ATPases inhibitor</li> </ul>	<i>C. albicans</i> : AmpB, CF <i>C. neoformans</i> : AmpB <i>S. cerevisiae</i> : AmpB, Ben, CF, FL, TB
Tomatidine	<ul style="list-style-type: none"> <li>• Antifungal</li> </ul>	<i>C. albicans</i> : Ben, CF, Cyp, FL, TB <i>C. neoformans</i> : FL <i>S. cerevisiae</i> : Ben, CF, Cyp, FL, TB <i>S. pombe</i> : FL, TB

**Table S5. ACM compound chemical interactions with antifungals. Calculated Fractional Inhibitory Concentration Index.** Related to Figure 3.

Strain	ACM Compound	MIC ACM Compound ( $\mu\text{M}$ )	FIC <sup>1</sup> ACM Compound	MIC caspofungin ( $\mu\text{g/mL}$ )	FIC <sup>1</sup> caspofungin	FIC Index <sup>2</sup>
<i>C. albicans</i>	AHC	25	0.13	0.5	0.13	0.3
<i>C. albicans</i>	Asiatic Acid	50	0.13	0.5	0.06	0.2
<i>C. albicans</i>	Clofazimine	$\geq 100$	0.03	0.5	0.13	0.2
<i>C. albicans</i>	Cyclosporin A	$\geq 50$	0.06	0.5	0.06	0.1
<i>C. albicans</i>	PCC	25	0.5	0.5	0.5	1
<i>C. albicans</i>	Suloctidil	$\geq 100$	0.5	0.5	0.06	0.6
<i>C. albicans</i>	Thapsigargin	$\geq 50$	0.5	0.5	0.06	0.6
<i>C. albicans</i>	Tomatidine	25	0.5	0.5	0.06	0.6
<i>S. cerevisiae</i>	AHC	6.25	0.25	0.5	0.06	0.3
<i>S. cerevisiae</i>	Asiatic Acid	$\geq 50$	0.25	0.5	0.13	0.4
<i>S. cerevisiae</i>	Clofazimine	$\geq 100$	0.03	0.5	0.06	0.1
<i>S. cerevisiae</i>	Cyclosporin A	$\geq 50$	0.06	0.5	0.06	0.1
<i>S. cerevisiae</i>	PCC	6.25	0.5	0.5	0.25	0.8
<i>S. cerevisiae</i>	Suloctidil	25	0.5	0.5	0.06	0.6
<i>S. cerevisiae</i>	Thapsigargin	$\geq 50$	0.5	0.5	0.06	0.6
<i>S. cerevisiae</i>	Tomatidine	12.5	0.25	0.5	0.25	0.5
<i>S. pombe</i>	AHC	6.25	0.5	4	0.5	1
<i>S. pombe</i>	Asiatic Acid	50	1	4	0.5	1.5
<i>S. pombe</i>	Clofazimine	$\geq 100$	0.5	4	0.13	0.6
<i>S. pombe</i>	Cyclosporin A	$\geq 50$	0.06	4	0.25	0.3
<i>S. pombe</i>	PCC	6.25	0.5	4	0.25	0.8
<i>S. pombe</i>	Suloctidil	12.5	0.5	4	0.02	0.5
<i>S. pombe</i>	Thapsigargin	$\geq 50$	1	4	1	2
<i>S. pombe</i>	Tomatidine	3.125	0.5	4	0.13	0.6
<i>C. neoformans</i>	AHC	6.25	0.5	$\geq 4$	0.5	1
<i>C. neoformans</i>	Asiatic Acid	25	2	$\geq 4$	0.5	2.5
<i>C. neoformans</i>	Clofazimine	$\geq 100$	0.25	$\geq 4$	0.13	0.4
<i>C. neoformans</i>	Cyclosporin A	$\geq 50$	1	$\geq 4$	1	2
<i>C. neoformans</i>	PCC	12	1	$\geq 4$	1	2
<i>C. neoformans</i>	Suloctidil	50	0.5	$\geq 4$	0.5	1
<i>C. neoformans</i>	Thapsigargin	$\geq 50$	1	$\geq 4$	1	2
<i>C. neoformans</i>	Tomatidine	25	1	$\geq 4$	1	2
Strain	ACM Compound	MIC ACM Compound ( $\mu\text{M}$ )	FIC <sup>1</sup> ACM Compound	MIC fluconazole ( $\mu\text{g/mL}$ )	FIC <sup>1</sup> fluconazole	FIC Index <sup>2</sup>
<i>C. albicans</i>	AHC	25	0.5	2	1	1.5
<i>C. albicans</i>	Asiatic Acid	50	0.5	2	1	1.5
<i>C. albicans</i>	Clofazimine	$\geq 100$	1	2	1	2
<i>C. albicans</i>	Cyclosporin A	$\geq 50$	0.5	2	0.5	1
<i>C. albicans</i>	PCC	25	0.5	2	0.25	0.8
<i>C. albicans</i>	Suloctidil	$\geq 100$	0.5	2	0.5	1
<i>C. albicans</i>	Thapsigargin	$\geq 50$	1	2	1	2
<i>C. albicans</i>	Tomatidine	25	0.13	2	0.25	0.4
<i>S. cerevisiae</i>	AHC	6.25	0.5	32	0.5	1

<i>S. cerevisiae</i>	Asiatic Acid	$\geq 50$	1	32	1	2
<i>S. cerevisiae</i>	Clofazimine	$\geq 100$	0.06	32	0.25	0.3
<i>S. cerevisiae</i>	Cyclosporin A	$\geq 50$	1	32	1	2
<i>S. cerevisiae</i>	PCC	6.25	0.5	32	0.13	0.6
<i>S. cerevisiae</i>	Suloctidil	25	0.5	32	0.02	0.5
<i>S. cerevisiae</i>	Thapsigargin	$\geq 50$	0.5	32	0.5	1
<i>S. cerevisiae</i>	Tomatidine	12.5	0.25	32	0.03	0.3
<i>S. pombe</i>	AHC	6.25	0.5	64	0.5	1
<i>S. pombe</i>	Asiatic Acid	50	1	64	1	2
<i>S. pombe</i>	Clofazimine	$\geq 100$	0.5	64	0.25	0.8
<i>S. pombe</i>	Cyclosporin A	$\geq 50$	1	64	1	2
<i>S. pombe</i>	PCC	6.25	0.5	64	0.5	1
<i>S. pombe</i>	Suloctidil	12.5	0.5	64	0.02	0.5
<i>S. pombe</i>	Thapsigargin	$\geq 50$	1	64	1	2
<i>S. pombe</i>	Tomatidine	3.125	0.5	64	0.13	0.6
<i>C. neoformans</i>	AHC	6.25	0.5	16	0.02	0.5
<i>C. neoformans</i>	Asiatic Acid	25	1	16	1	2
<i>C. neoformans</i>	Clofazimine	$\geq 100$	0.25	16	0.13	0.4
<i>C. neoformans</i>	Cyclosporin A	$\geq 50$	1	16	1	2
<i>C. neoformans</i>	PCC	12	1	16	1	2
<i>C. neoformans</i>	Suloctidil	50	0.5	16	0.06	0.6
<i>C. neoformans</i>	Thapsigargin	$\geq 50$	1	16	1	2
<i>C. neoformans</i>	Tomatidine	25	0.25	16	0.06	0.3

<sup>1</sup> Fractional Inhibitory Concentration (FIC) = [X]/MIC<sub>x</sub>, where [X] is the lowest inhibitory concentration of drug in the presence of the co-drug.

<sup>2</sup> FIC index = FIC<sub>ACM compound</sub> + FIC<sub>antifungal</sub>

**Table S6. Dataset for Haploinsufficiency Profiling and Homozygous Deletion Profiling. Calculated Z-scores from all diploid and haploid deletion strain sensitivity profile.** Related to Figure 5.

**Table S7. Strains used in this study.** Related to Figure 1.

Strain Name	Description	Genotype	Source
<b>GDW39</b>	<i>C. albicans</i> NCCLS 11	Wild type	ATCC # 90028
<b>GDW361</b>	<i>S. cerevisiae</i> BY4741	<i>MAT a his3Δ leu2Δ met15Δ ura3Δ</i>	(Giaever et al., 2002)
<b>GDW508</b>	<i>C. albicans</i> Y537	Amphotericin B Resistant Clinical Isolate	ATCC # 200955
<b>GDW509</b>	<i>C. tropicalis</i>	Wild type	ATCC # 200956
<b>GDW655</b>	<i>C. neoformans</i> H99	Wild type	Strain received from James W. Kronstad
<b>GDW1004</b>	<i>S. pombe</i>	Wild type	ATCC # 38366
<b>GDW1584</b>	<i>C. parapsilosis</i>	Wild type	ATCC # 22019
<b>GDW1585</b>	<i>C. albicans</i> Fluconazole Resistant Clinical Isolate	CAP-F-1-2008 LL#99383	Deborah Yamamura, St Joseph's Hospital, Hamilton ON
<b>GDW1586</b>	<i>C. albicans</i> Fluconazole Resistant Clinical Isolate	CAP-F-07-2007 LL#99359	Deborah Yamamura, St Joseph's Hospital, Hamilton ON
<b>GDW1587</b>	<i>C. glabrata</i>		Deborah Yamamura, St Joseph's Hospital, Hamilton ON
<b>GDW2295</b>	<i>A. fumigatus</i> Af293	Wild type	(Nierman et al. 2005)
<b>GDW2590</b>	<i>C. albicans</i> , SN95	<i>arg4Δ/arg4Δhis1Δ/his1Δ URA3/ura3Δ::imm434 IRO1/iro1Δ::imm434</i>	(Noble, SM and Johnson AD. 2005)
<b>GDW2592</b>	<i>C. albicans</i> <i>pkc1/pkc1</i>	As SN95, <i>CaTAR::HIS3 pkc1::FRT/ pkc1::FRT</i>	(Lafayette et. al.2010)
<b>GDW2593</b>	<i>C. albicans</i> <i>pkc1Δ/pkc1Δ + PKC1</i>	As SN95, <i>CaTAR::HIS3 pkc1::FRT/ pkc1::FRT::CaPKC1-FRT</i>	(Lafayette et. al.2010)
<b>GDW2597</b>	<i>S. cerevisiae</i> , SLT2-GFP	<i>MAT a his3Δ leu2Δ met15Δ ura3Δ</i>	(Huh, W-K et al. 2003)
<b>Sc bck1</b>	<i>S. cerevisiae</i> BY4741 <i>bck1Δ</i>	As BY4741, <i>bck1::KAN</i>	Homozygous Deletion Library
<b>Sc dfg16</b>	<i>S. cerevisiae</i> BY4741 <i>dfg16Δ</i>	As BY4741, <i>dfg16::KAN</i>	Homozygous Deletion Library

<b>Sc <i>mkk2</i></b>	<i>S. cerevisiae</i> BY4741 <i>mkk2Δ</i>	As BY4741, <i>mkk2::KAN</i>	Homozygous Deletion Library
<b>Sc <i>PKC1/pkc1</i></b>	<i>S. cerevisiae</i> BY4743 <i>PKC1/pkc1Δ</i>	As BY4743, <i>PKC1/pkc1::KAN</i>	Heterozygous Deletion Library
<b>Sc <i>rim101</i></b>	<i>S. cerevisiae</i> BY4741 <i>rim101Δ</i>	As BY4741, <i>rim101::KAN</i>	Homozygous Deletion Library
<b>Sc <i>rim13</i></b>	<i>S. cerevisiae</i> BY4741 <i>rim13Δ</i>	As BY4741, <i>rim13::KAN</i>	Homozygous Deletion Library
<b>Sc <i>rim20</i></b>	<i>S. cerevisiae</i> BY4741 <i>rim20Δ</i>	As BY4741, <i>rim20::KAN</i>	Homozygous Deletion Library
<b>Sc <i>rim21</i></b>	<i>S. cerevisiae</i> BY4741 <i>rim21Δ</i>	As BY4741, <i>rim21::KAN</i>	Homozygous Deletion Library
<b>Sc <i>rim8</i></b>	<i>S. cerevisiae</i> BY4741 <i>rim8Δ</i>	As BY4741, <i>rim8::KAN</i>	Homozygous Deletion Library
<b>Sc <i>rlm1</i></b>	<i>S. cerevisiae</i> BY4741 <i>rlm1Δ</i>	As BY4741, <i>rlm1::KAN</i>	Homozygous Deletion Library
<b>Sc <i>slt2</i></b>	<i>S. cerevisiae</i> BY4741 <i>slt2Δ</i>	As BY4741, <i>slt2::KAN</i>	Homozygous Deletion Library
<b>Sc <i>swi4</i></b>	<i>S. cerevisiae</i> BY4741 <i>swi4Δ</i>	As BY4741, <i>swi4::KAN</i>	Homozygous Deletion Library
<b>Sc <i>swi6</i></b>	<i>S. cerevisiae</i> BY4741 <i>swi6Δ</i>	As BY4741, <i>swi6::KAN</i>	Homozygous Deletion Library

**Table S8. Oligonucleotides used in this study.** Related to Figure 4 and Figure 5.

## SUPPLEMENTAL EXPERIMENTAL PROCEDURES

### Strains and Culture Conditions

Archives of *C. albicans* and *S. cerevisiae* were maintained at -80C in 25% glycerol.

Strains were grown in either synthetic complete medium (SC: 0.67% Difco™ yeast nitrogen base w/o amino acids, 0.08% amino acid add back and 2% glucose) or in yeast peptone dextrose (YPD, 1% yeast extract, 2% bactopeptone, 2% glucose) as indicated.

2% agar was added for solid media. Strains used in this study are listed in Table S7.

## High-Throughput Screening Conditions

The McMaster Bioactives collection, a compilation of chemicals purchased from Prestwick, Biomol, Sigma, and Microsource, was screened at a final concentration of 12.5  $\mu\text{M}$  in the presence and absence of  $\frac{1}{4}$  MIC antifungal (Amphotericin B, Benomyl, Caspofungin, Cyprodinil, Fluconazole and Terbinafine). Screens were performed using *C. albicans* (ATCC 90028), *C. neoformans* (H99), *S. cerevisiae* (BY4741), and *S. pombe* (ATCC 38366). For each assay plate, the 32 high and 32 low growth controls were used to calculate residual growth within each well on the same assay plate as follows:

$$RG = ((A_{600} - (\mu - c)) \div ((\mu + c) - (\mu - c)))$$

where  $\mu+c$ , and  $\mu-c$  are the  $A_{600}$  averages of the high-growth (+c) and low-growth (-c) controls. The robustness of the screen was measured by calculating the  $Z'$  score and all screens achieved a  $Z'$  above 0.5 indicating an adequate screening window (Zhang, Chung et al. 1999). Screens were conducted in duplicate in 384-well flat bottom microtitre plates (ThermoScientific) with a final volume of 80  $\mu\text{L}$ . A Beckman Biomek FX liquid handler (Beckman Coulter Inc., Fullerton, CA) was used to dispense 1  $\mu\text{L}$  of McMaster Bioactive compound at a 1mM concentration and 1  $\mu\text{L}$  of antifungal at 80X concentration used for the screen. This was followed by the addition of 78  $\mu\text{L}$  of diluted cell culture prepared in SC. For preparation of diluted yeast culture, liquid overnight cultures in were diluted to an  $OD_{600}$  of 0.14, followed by a 1:1000 dilution in SC media. Positive growth controls (DMSO only) and negative growth controls (antifungal above the MIC) were included in rows 1, 2, 23 and 24 of each plate for normalization. Plates were incubated at 30°C. The  $OD_{600}$  was measured after 48 h of growth for *S. cerevisiae*

and *C. albicans* or 72 h of growth for *C. neoformans* and *S. pombe*. Growth controls on each plate were used to generate percentage growth data, and replicates were plotted against each other to identify outliers. All data was normalized for plate- and row/column-specific effects as described previously (Spitzer, Griffiths et al. 2011). To identify compounds that potentiated antifungals, growth in the presence of the antifungal was plotted against growth in the absence of the antifungal and data was fit to a linear model. Hits were considered those compounds that were 3 median absolute deviations (MADs) below the diagonal, inhibited growth on their own less than 50%, and resulted in at least 80% growth inhibition in the presence of the antifungal. Chemical-chemical interactions were generated using the program Cytoscape v3.2.1 (<http://www.cytoscape.org>).

### **Drug Susceptibility Assays**

MIC and checkerboard assays were performed in U-bottom, 96-well microtiter plates (Fisher Scientific) using a modified broth microdilution protocol as described (LaFayette et al., 2010). In brief, assays were set up in SC media in a total volume of 0.2 mL/well with 2-fold dilutions of drug. Plates were incubated in the dark for 48 h-72 h, and absorbance was determined at 600 nm using a spectrophotometer (Molecular Devices). Each strain was tested in duplicate on at least two occasions. Data was quantitatively displayed with color using the program Java TreeView 1.1.6 (<http://jtreeview.sourceforge.net>). For growth curve analysis, overnight cultures were diluted to OD<sub>600</sub> of 0.0625 with or without compound as indicated and grown at 30°C with continuous shaking, using the TECAN Sunrise. Optical density was measured at

595 nm every 15 min over 24 h – 48 h. Data was plotted and analyzed using GraphPad Prism.

### **Sequencing Analysis for Chemical Genomic Assays**

The Illumina MiSeq platform and MiSeq Reagent kit v3 (2 x 75 bp) were used for sequencing. To avoid problems with cluster identification due to low diversity during the first 18 cycles, which correspond to the common deletion strain primer sequences, we started the run with 'dark cycle sequencing' through these first 18 nucleotides (sequencing chemistry occurs, but no imaging). Next Gen sequencing data were trimmed and counted with R scripts. PatMaN software was used to match sequences to barcodes (Prufer, Stenzel et al. 2008). All sequences with up to 3 mismatches to barcodes were kept. Log2 ratios of compound-treated versus DMSO-treated samples were generated and data was normalized by calculating Z-scores.

### **Sequencing of Fluconazole-Resistant Isolate of *C. albicans***

The fluconazole-resistant isolate of *C. albicans* was grown in YPD medium to late log-phase at which time gDNA was extracted using phenol-chloroform extraction methods. *ERG11*, *TAC1* and *UPC2* were amplified using primer combination indicated in Table S8. PCR products were sent for sequencing at the Farncombe Metagenomics Facility at McMaster University. Sequencing results were aligned relative to reference sequences obtained from *C. albicans* SC5314 Assembly 22.

### **Murine Model of *C. albicans* Infection.**

For murine exposure, male CD1 mice (Charles River Laboratories) aged 5-6 weeks (20-25 g) were infected via the tail vein with 200 µl of a  $1 \times 10^6$  CFU/ml PBS suspension of *C. albicans* SC5314. Each treatment group consisted of 5 mice. Fluconazole is purchased from the Duke Pharmacy Storeroom (Pfizer, 16 mg/kg) and caspofungin, also from Duke Pharmacy, (Merck, 0.1 mg/kg) were administered i.p. whereas clofazimine (Sigma, 5 mg/kg) was administered by oral gavage. Drugs were given injected at 4 h, 24 h, 48 h, and 72 h post infection. Mice were observed daily for signs of illness. All murine work was performed under a protocol, approved by the Institutional Animal Use and Care Committee at Duke University Medical Center.

### **Ethics Statement**

Animals studies were conducted in the Division of Laboratory Animal Resources (DLAR) facilities at Duke University Medical Center (DUMC) in good practice as defined by the United States Animal Welfare Act and in full compliance with the guidelines of the DUMC Institutional Animal Care and Use Committee (IACUC). The vertebrate animal experiments were reviewed and approved by the DUMC IACUC under protocol number A114-14-05.

### **SUPPLEMENTAL REFERENCES**

Giaever, G., A. M. Chu, L. Ni, C. Connelly, L. Riles, S. Veronneau, S. Dow, A. Lucau-Danila, K. Anderson, B. Andre, A. P. Arkin, A. Astromoff, M. El-Bakkoury, R. Bangham, R. Benito, S. Brachat, S. Campanaro, M. Curtiss, K. Davis, A. Deutschbauer, K. D. Entian, P. Flaherty, F. Foury, D. J. Garfinkel, M. Gerstein,

D. Gotte, U. Guldener, J. H. Hegemann, S. Hempel, Z. Herman, D. F. Jaramillo, D. E. Kelly, S. L. Kelly, P. Kotter, D. LaBonte, D. C. Lamb, N. Lan, H. Liang, H. Liao, L. Liu, C. Luo, M. Lussier, R. Mao, P. Menard, S. L. Ooi, J. L. Revuelta, C. J. Roberts, M. Rose, P. Ross-Macdonald, B. Scherens, G. Schimmack, B. Shafer, D. D. Shoemaker, S. Sookhai-Mahadeo, R. K. Storms, J. N. Strathern, G. Valle, M. Voet, G. Volckaert, C. Y. Wang, T. R. Ward, J. Wilhelmy, E. A. Winzeler, Y. Yang, G. Yen, E. Youngman, K. Yu, H. Bussey, J. D. Boeke, M. Snyder, P. Philippsen, R. W. Davis and M. Johnston (2002). "Functional profiling of the *Saccharomyces cerevisiae* genome." Nature **418**(6896): 387-391.

Huh, W. K., J. V. Falvo, L. C. Gerke, A. S. Carroll, R. W. Howson, J. S. Weissman and E. K. O'Shea (2003). "Global analysis of protein localization in budding yeast." Nature **425**(6959): 686-691.

LaFayette, S. L., C. Collins, A. K. Zaas, W. A. Schell, M. Betancourt-Quiroz, A. A. Gunatilaka, J. R. Perfect and L. E. Cowen (2010). "PKC signaling regulates drug resistance of the fungal pathogen *Candida albicans* via circuitry comprised of Mkc1, calcineurin, and Hsp90." PLoS Pathog **6**(8). e1001069

Nierman, W. C., A. Pain, M. J. Anderson, J. R. Wortman, H. S. Kim, J. Arroyo, M. Berriman, K. Abe, D. B. Archer, C. Bermejo, J. Bennett, P. Bowyer, D. Chen, M. Collins, R. Coulsen, R. Davies, P. S. Dyer, M. Farman, N. Fedorova, N. Fedorova, T. V. Feldblyum, R. Fischer, N. Fosker, A. Fraser, J. L. Garcia, M. J. Garcia, A. Goble, G. H. Goldman, K. Gomi, S. Griffith-Jones, R. Gwilliam, B. Haas, H. Haas, D. Harris, H. Horiuchi, J. Huang, S. Humphray, J. Jimenez, N. Keller, H. Khouri, K. Kitamoto, T. Kobayashi, S. Konzack, R. Kulkarni, T.

Kumagai, A. Lafon, J. P. Latge, W. Li, A. Lord, C. Lu, W. H. Majoros, G. S. May, B. L. Miller, Y. Mohamoud, M. Molina, M. Monod, I. Mouyna, S. Mulligan, L. Murphy, S. O'Neil, I. Paulsen, M. A. Penalva, M. Pertea, C. Price, B. L. Pritchard, M. A. Quail, E. Rabbinowitsch, N. Rawlins, M. A. Rajandream, U. Reichard, H. Renauld, G. D. Robson, S. Rodriguez de Cordoba, J. M. Rodriguez-Pena, C. M. Ronning, S. Rutter, S. L. Salzberg, M. Sanchez, J. C. Sanchez-Ferrero, D. Saunders, K. Seeger, R. Squares, S. Squares, M. Takeuchi, F. Tekaia, G. Turner, C. R. Vazquez de Aldana, J. Weidman, O. White, J. Woodward, J. H. Yu, C. Fraser, J. E. Galagan, K. Asai, M. Machida, N. Hall, B. Barrell and D. W. Denning (2005). "Genomic sequence of the pathogenic and allergenic filamentous fungus *Aspergillus fumigatus*." Nature **438**(7071): 1151-1156.

Noble, S. M. and A. D. Johnson (2005). "Strains and strategies for large-scale gene deletion studies of the diploid human fungal pathogen *Candida albicans*." Eukaryot Cell **4**(2): 298-309.

Prufer, K., U. Stenzel, M. Dannemann, R. E. Green, M. Lachmann and J. Kelso (2008). "PatMaN: rapid alignment of short sequences to large databases." Bioinformatics **24**(13): 1530-1531.

Spitzer, M., E. Griffiths, K. M. Blakely, J. Wildenhain, L. Ejim, L. Rossi, G. De Pascale, J. Curak, E. Brown, M. Tyers and G. D. Wright (2011). "Cross-species discovery of syncretic drug combinations that potentiate the antifungal fluconazole." Mol Syst Biol **7**: 499.

Zhang, J. H., T. D. Chung and K. R. Oldenburg (1999). "A Simple Statistical Parameter for Use in Evaluation and Validation of High Throughput Screening Assays." J Biomol Screen 4(2): 67-73.